PENSOFT
SENCKENBERG world of biodiversity
Leibniz Association

A new species of *Brachycephalus* (Anura: Brachycephalidae) from the northern portion of the state of Rio de Janeiro, southeastern Brazil

Manuella Folly[1], Thais H. Condez[2], Davor Vrcibradic[3], Carlos F. D. Rocha[4], Alessandra S. Machado[5], Ricardo T. Lopes[5], José P. Pombal Jr.[1]

1 *Departamento de Vertebrados, Museu Nacional, Universidade Federal do Rio de Janeiro, Av. Bartolomeu de Gusmão, 875, São Cristóvão, 20941-160 Rio de Janeiro, Brazil*

2 *Department of Earth Sciences, Carleton University, 1125 Colonel By Drive, K1S5B6 Ottawa, Ontario, Canada*

3 *Departamento de Zoologia, Universidade Federal do Estado do Rio de Janeiro, Av. Pasteur 458, Urca, 22240-290 Rio de Janeiro, Brazil*

4 *Departamento de Ecologia, Universidade do Estado do Rio de Janeiro, Rua São Francisco Xavier 524, Maracanã, 20550-013 Rio de Janeiro, Brazil*

5 *Instituto Alberto Luiz Coimbra de Pós-graduação e Pesquisa em Engenharia, Laboratório de Instrumentação Nuclear, Universidade Federal do Rio de Janeiro, 21941-450 Rio de Janeiro, Brazil*

http://zoobank.org/83AB34EE-9D5D-4F47-9536-0A4D1EB60568

Corresponding author: Manuella Folly (follymga@gmail.com)

Academic editors Raffael Ernst / Deepak Veerappan | **Received** 6 March 2023 | **Accepted** 6 December 2023 | **Published** 16 January 2024

Citation: Folly M, Condez TH, Vrcibradic D, Rocha CFD, Machado AS, Lopes RT, Pombal Jr JP (2024) A new species of *Brachycephalus* (Anura, Brachycephalidae) from the northern portion of the state of Rio de Janeiro, southeastern Brazil. Vertebrate Zoology 74 1–21. https://doi.org/10.3897/vz.74.e103573

Abstract

Brachycephalus is a genus of small ground-dwelling anurans, endemic to the Brazilian Atlantic Forest. Recent molecular analyses have corroborated the monophyly of three species groups within this genus (*B. ephippium*, *B. pernix*, and *B. vertebralis*). In the meantime, the genus has been targeted as a group with recent taxonomic issues owing to its interspecific morphological similarity and genetic conservatism. Herein, we describe a new species of *Brachycephalus* from the northern portion of Serra do Mar mountain range, in the state of Rio de Janeiro, Brazil. It belongs to the *B. vertebralis* species group, exhibiting moderate hyperossification of the skull and vertebral column. The new species can be distinguished from all other congeners based on morphological, acoustic, and molecular data. Furthermore, we provide information on osteology and natural history of the new species.

Keywords

Atlantic Forest, Brachycephaloidea, osteology, pumpkin toadlet, Serra do Mar

Introduction

The Neotropical anuran family Brachycephalidae currently comprises two genera: *Brachycephalus* Fitzinger, 1826 and *Ischnocnema* Reinhardt & Lütken, 1862. The latter comprises species varying in body size (snout–vent length) from less than 20 mm to more than 50 mm, whereas the former contains only miniaturized species less than 20 mm in snout–vent length (Hedges et al. 2008; Condez et al. 2021). The genus *Brachycephalus*

is endemic to the Brazilian Atlantic Forest and currently comprises 40 species, ten of which were described within the last five years (see Frost 2023). Species within the genus *Brachycephalus* exhibit a high degree of local endemism, with more than half of them (21 species) being known only from their type locality (e.g., *B. guarani* Clemente-Carvalho et al., 2012; *B. crispus* Condez, Clemente-Carvalho, Haddad & Reis, 2014; *B. puri* Almeida-Silva, Silva-Soares, Rodrigues & Verdade, 2021; *B. tabuleiro* Mângia et al., 2023), and eleven species being known only from their type locality and its surroundings (e.g., *B. pitanga* Alves, Sawaya, Reis & Haddad, 2009; *B. margaritatus* Pombal & Izecksohn, 2011; *B. actaeus* Monteiro et al., 2018; *B. clarissae* Folly et al., 2022).

The first published phylogenetic hypothesis focused on *Brachycephalus* (Clemente-Carvalho et al. 2011), based on all 14 species known at the time, indicated the existence of two main clades: one containing the brightly-colored species with hyperossification of skull and skeleton and the other containing the brightly-colored non-hyperossified ones; however, the relationships of the two cryptically colored species formerly included in the genus *Psyllophryne* Izecksohn, 1971 (see Kaplan 2002) were not consistent, with *B. hermogenesi* (Giaretta & Sawaya, 1998), in particular, being recovered in different positions in different gene trees (always with strong support, and usually within one of the brightly-colored species groups). Subsequently, it was proposed to allocate the species of *Brachycephalus* into three species groups based on morphological characters: the *B. didactylus*, *B. ephippium*, and *B. pernix* groups (Pie and Ribeiro 2015; Ribeiro et al. 2015; Bornschein et al. 2016). However, recent molecular phylogenetic studies, recovered only two of these groups as monophyletic (the *B. ephippium* and *B. pernix* groups), while species previously assigned to the *B. didactylus* group were not recovered as a clade (e.g., Condez et al. 2020; Folly et al. 2020, 2022; Dos Reis et al. 2021; Almeida-Silva et al. 2021). Lyra et al. (2021) recovered a similar topology in a phylogenomic study including nine *Brachycephalus* species.

More recently, Folly et al. (2022) reappraised the species groups within *Brachycephalus*, specifically dividing the *B. ephippium* species group into two distinct groups (previously referred to as lineages by Condez et al. 2020) based on solid phylogenetic relationships and osteological characters (Condez et al. 2020; Folly et al. 2020; Dos Reis et al. 2021): (1) the *B. vertebralis* species group, with ossification at the distal end of the fourth vertebral process (moderate condition of skull and skeletal hyperossification), including *B. alipioi* Pombal & Gasparini, 2006, *B. bufonoides* Miranda-Ribeiro, 1920, *B. crispus*, *B. guarani*, *B. nodoterga* Miranda-Ribeiro, 1920, *B. pitanga*, *B. toby* Haddad, Alves, Clemente-Carvalho & Reis, 2010, and *B. vertebralis* Pombal, 2001; and (2) the *B. ephippium* species group, with cranial and dorsal bony plates (extreme condition of skull and skeletal hyperossification), including *B. darkside* Guimarães, Luz, Rocha & Feio, 2017, *B. ephippium* (Spix, 1824), *B. garbeanus* Miranda-Ribeiro, 1920, *B. ibitinga* Condez et al., 2021, *B. margaritatus*, and *B. rotenbergae* Nunes et al., 2021. As suggested by Folly et al. (2021a, 2022), we do not consider the *B. didactylus* species group due to its non-monophyly. Therefore, the following species of *Brachycephalus* are not attributed to any species group and will be herein collectively referred as "flea-toads": *B. clarissae*, *B. didactylus* (Izecksohn, 1971), *B. hermogenesi*, *B. pulex* Napoli, Caramaschi, Cruz & Dias, 2011, *B. puri*, and *B. sulfuratus* Condez et al., 2016.

Herein, we describe a new species of *Brachycephalus* belonging to the *B. vertebralis* species group (sensu Folly et al. 2022), from the Parque Estadual do Desengano, municipality of Santa Maria Madalena, northern portion of the state of Rio de Janeiro, Brazil. The new species' description is based on an integrative approach, involving morphological (including osteological features), molecular, and bioacoustic data analyses.

Material and Methods

Morphological data

For morphometrics, a single person (M. Folly) took 18 measurements (in mm) from each of the 17 collected specimens with an ocular micrometer in a Leica MZ-6 stereomicroscope (0.01 mm): snout–vent length (**SVL**; ventral distance from the tip of the snout to cloacal opening); head length (**HL**; dorsal distance from the tip of the snout to angle of jaw); head width (**HW**; greatest width of head located between angles of jaw); nostril diameter (**ND**; maximum width of the nostril); inter-nostril distance (**IND**; taken between inner margins of nostrils); nostril–tip of snout distance (**NSD**; from anterior margin of nostril to the tip of the snout); interorbital distance (**IOD**; interval between the inner edges of the orbits); eye diameter (**ED**); eyelid width (**EW**); eye-nostril distance (**END**; from anterior corner of the eye to posterior margin of nostril); arm length (**AL**; distance between axilla and elbow); forearm length (**FAL**; distance between elbow and wrist); hand length (**HAL**; distance between the wrist and the tip of Finger III); Finger-III length (**FIL**; insertion between Fingers II–III to the tip of Finger III); thigh length (**THL**; distance from the cloaca to the knee); shank length (**SL**; distance from the ankle to the knee); foot length (**FL**; distance between the ankle and the tip of Toe III); and Toe-III length (**TL**; insertion between Toes II–III to the tip of Toe III). Except for FL, which is modified to include tarsus length, all these measurements follow Duellman (1970), Cei (1980), and Heyer et al. (1990). Some measurements (ND, NSD, ED, FIL, and TL) were also included because they are informative and currently adopted by taxonomists working with the genus *Brachycephalus* (Condez et al. 2016). The sex of specimens was determined by gonad examination. To evaluate sexual dimorphism, we tested differences in body size between males and females using the T-test (R Core Team 2022). For comparisons with other species in the genus we used data both from specimens examined in collections (see

Table S1) and from the literature (especially original descriptions and redescriptions of taxa). We followed Sabaj (2016) for museum acronyms. Descriptive terminology of the snout follows Heyer et al. (1990). The fingers were numbered II–V following Fabrezi and Alberch (1996).

One adult specimen (MNRJ 42407) was cleared and double-stained for osteological observations, following the methods of Taylor and Van Dyke (1985), with few modifications. Two males (CFBH 28048 and 28133), and two females (CFBH 28131 and 28137) were CT-scanned on a Skyscan/Bruker equipment, model 1173 available in the Nuclear Instrumentation Laboratory, COPPE, at the Universidade Federal do Rio de Janeiro. The images were obtained in a voltage and current of 40 kV and 190 μA, respectively. Terminology of cranial osteology follows Campos et al. (2010) and Trueb (2015); hyolaryngeal skeleton follows Trewavas (1933); pectoral girdle follows Trueb (1973); that of manus and pes follow Fabrezi (1992, 1993, 2001); and vertebral column follows Campos et al. (2010). The resulting files were archived on MorphoSource.org database (available at http://morphosource.org), with the following ID numbers: CFBH 28048 (ID: 000588996), CFBH 28133 (ID: 000589012), CFBH 28131 (ID: 000589003). and CFBH 28137 (ID: 000589019).

Molecular data and phylogenetic analysis

In this study, we obtained novel molecular information from nine specimens within the new species. Three mitochondrial gene segments were selected: 12S ribosomal RNA (12S rRNA), 16S ribosomal RNA (16S rRNA), and cytochrome *b* (cyt *b*). GenBank accession numbers are listed in Table S2. We performed PCRs using a PCR Master Mix and a pair of primers for each gene segment, respectively listed here: 12SJL forward (AAAGRTTTGGTCCTRRSCTT) and 12SKH reverse (TCCRGTAYRCTTACCDTGTTACGA) published in Goebel et al. (1999); 12SM forward (GGCAAGTCGTAACATGGTAAG) and 16SA reverse (ATGTTTTTGGTAAACAGGCG) published in Darst and Cannatella (2004); MVZ15-L forward (GAACTAATGGCCCACACWWTACGNAA) published in Moritz et al. (1992) and CytbAR-H reverse (TAWAAGGGTCTTCTACTGGTTG) published in Goebel et al. (1999). Thermocycling conditions for 12S rRNA and 16S rRNA amplification began with a denaturation at 94 °C (5 min), followed by 35 cycles of denaturation at 94 °C (1 min), annealing at 50–52 °C (1 min), and a final extension step at 72 °C after the final cycle (5 min). Amplification conditions for cyt *b* were the same as described above, except that the annealing temperatures were adjusted to primer-specific temperatures ranging from 50 to 55 °C. PCR products were visualized in 1% agarose gels and sent to Macrogen Inc. (Seoul, Republic of Korea) for purification and sequencing reactions. Resulting electropherograms for both DNA strands were analyzed using Chromas Lite 2.01 and edited using MEGA X and adjusted manually to generate consensus sequences for each specimen. Sequences were checked with basic local alignment search tool (Altschul et al. 1997) against the GenBank nucleotide database to ensure that the amplified product was correct and not contaminated. We also confirmed the authenticity of the cyt *b* gene fragment by amino acid translations.

We complemented our sampling with available sequences from the GenBank database (Table S2). Our database comprises molecular information for 126 terminals, including the currently known diversity within the *Brachycephalus vertebralis* species group and several candidate species (Condez et al. 2020). We used *Pristimantis savagei* (Pyburn & Lynch, 1981) (Strabomantidae: Pristimantinae) to root the tree, and the outgroup taxa: *Oreobates quixensis* Jiménez de la Espada, 1872 (Strabomantidae: Pristimantinae), *Holoaden bradei* Lutz, 1958 (Strabomantidae: Holoadeninae), in addition to *Ischnocnema guentheri* (Steindachner, 1864), *I. holti* (Cochran, 1948), *I. parva* (Girard, 1853), and *I. verrucosa* (Reinhardt & Lütken, 1862) (Brachycephalidae), following recent systematic relationships within the new world direct-developing frogs (Padial et al. 2014; Heinicke et al. 2018).

Four mitochondrial gene segments were included in our analysis: 12S ribosomal RNA (12S rRNA, 826 bp), 16S ribosomal RNA (16S rRNA, 1548 bp), Cytochrome C oxidase subunit I (COI, 706 bp), and cytochrome *b* (cyt *b*, 691 bp); along with three nuclear gene segments: Recombination-activating protein 1 and 2 (RAG1, 691 bp; RAG2, 491 bp), and Tyrosinase (Tyr, 571 bp). Sequences were then aligned using MAFFT 7.402 (Katoh and Standley 2013). For 16S rRNA alignment we chose the Q-INS-i strategy that considers RNA secondary structure (Katoh and Toh 2008), the default transition-transversion cost ratio, and gap opening penalty. For other alignments, MAFFT automatically selected the L-INS-i accurate strategy. We concatenated mitochondrial and nuclear gene fragments using Sequence Matrix 1.0 (Vaidya et al. 2011).

We used PartitionFinder 2.1.1 (Lanfear et al. 2017) to select the optimal partition scheme and nucleotide substitution models for each fragment, except for the protein coding genes, which had individual codon positions treated as separated partitions. We adopted the corrected Akaike Information Criterion (AICc) to select the best-fitting model for each gene, considering all possible models (JC, K80, SYM, F81, HKY, and GTR, with +G, +I, and +I +G as additional parameters), linked branch lengths, and the greedy search algorithm. After this, we performed a Bayesian Inference analysis in MrBayes 3.2.6 (Ronquist et al. 2012), running two independent analyses with four chains each, adopting the Markov Chain Monte Carlo approach (MCMC). We ran 100 million generations, sampling every 10,000 generations, and discarding the first 25% of generations as burn-in. Parameter convergences were checked in Tracer 1.6 (Rambaut et al. 2014). Trees were summarized in a majority-rule consensus tree where the node support values correspond to the Posterior Probabilities. Tree topology was edited using FigTree 1.4.3 (Rambaut 2016) and Illustrator (Adobe Inc. 2019).

MAFFT, PartitionFinder and MrBayes analyses were run at the CIPRES Science Gateway Portal (Miller et al. 2010). Additionally, we calculated the uncorrected pairwise genetic distances (*p*-distances) within the new species sequences and among its related taxa. We conducted this analysis using Mega X (Kumar et al. 2018; Stecher et al. 2020), considering the pairwise deletion of gaps and missing data.

Advertisement call analysis

The advertisement call description was based on unvouchered recordings from Parque Estadual do Desengano, trail to Pico do Desengano, municipality of Santa Maria Madalena, state of Rio de Janeiro, Brazil (21°52'49.1"S, 41°55'0.9"W; 1167 m a.s.l.; WGS84). Three distinct calling males were recorded with a Marantz PMD-660 digital recorder coupled to an external unidirectional Sennheiser ME-66 microphone by T.H. Condez, on 22 February 2011 at 13:55 p.m. (28.5°C, 75% UR), and on 23 February 2011 respectively at 16:00 p.m. (20.1°C, 88% UR) and 16:40 p.m. (21.2°C, 81% UR). Recordings were made at 44.1 kHz sampling rate and sample size of 16 bit in the mono pattern. Even though no other species in the area has the same call characteristics, the taxonomic assignment was confirmed by the collection of specimens in the targeted area immediately after the recordings were taken. Sound files are deposited in Fonoteca Neotropical Jacques Vielliard, at Universidade Estadual de Campinas (respectively as **FNJV** 58772, 58773, and 58774). Prior to the analysis we tested 500–2000 Hz high-pass filters to sound files to try reducing the background noise using Audacity v2.1.1 (Audacity Team 2017). As we were still not able to analyze the oscillograms after background filtering, we kept the original recordings for subsequent analysis. We therefore recognize that further recordings are necessary to refine some of the temporal parameters presented for the advertisement call of this species. Bioacoustic analyses were performed using 20 calls per individual in the program Raven Pro 1.5 (Bioacoustics Research Program 2014). Spectrograms were produced with a Hann window type, window size 512 samples, overlap 90% (locked), hop size 51 samples, DFT size 1024 samples (locked), grid spacing 43.1 Hz, brightness and contrast in default, and color map Cool. We used the note-centered approach and quantified ten advertisement call parameters, according to Köhler et al. (2017; but see Hepp and Pombal 2019): (1) call duration (s), (2) inter-call interval (s), (3) number of notes per call (notes/call), (4) note repetition rate (notes/s), (5) number of pulses per note (pulses/note), (6) number of pulses/note (pulses/note), (7) pulse repetition rate (pulses/s), (8) dominant frequency (peak frequency in Raven Pro 1.5), (9) lower and (10) upper frequencies (kHz; frequency 5% and frequency 95% in Raven Pro 1.5, respectively). Values are presented as the parameter range plus the average ± standard deviation (in parenthesis). The sound graphics were prepared in R 4.0.1 (R Core Team 2020) using the package Seewave v2.1.0 (Sueur et al. 2008), with the spectrogram settings Hann window, 90% overlap, 256 samples resolution, and a color scale defined by 50 relative dB.

Results

Brachycephalus herculeus sp. nov.

https://zoobank.orgBA016993-4B11-4770-A245-7688E37823CE

Figure 1

Chresonymy.
Brachycephalus sp. – Siqueira et al. (2011)
Brachycephalus sp. 2 – Condez et al. (2020); Folly et al. (2022)

Holotype. MNRJ 42408, adult male, Parque Estadual do Desengano, vicinity of Estalagem Morumbeca, municipality of Santa Maria Madalena, state of Rio de Janeiro, Brazil (21°52'42.3"S, 41°55'11.9"W; 1100 m a.s.l.), collected by D. Vrcibradic on 3 June 2006.

Paratypes. MNRJ 42407, adult, cleared-and-stained specimen, collected with the holotype. MNRJ 42409, adult male, collected by C.C. Siqueira on 6 June 2006; MNRJ 42410, adult male, collected by H.G. Bergallo on May 2006, all in the same site as the holotype. MNRJ 52718, adult female, and MNRJ 52719–52721, adult males, Parque Estadual do Desengano, Estalagem Morumbeca, municipality of Santa Maria Madalena, state of Rio de Janeiro, Brazil (21°52′33″S, 41°55′08″W; 1050 m a.s.l.), collected by A. Chagas, A. Kury, C. Sampaio and T. Moreira, from 13–17 May 2008. CFBH 28049, adult female, CFBH 28124, 28129–30, 28135, adult males, and CFBH 28128, 28132–34, 28136–38, individuals of undetermined sex, including juveniles, Parque Estadual do Desengano, trail to Pico do Desengano, municipality of Santa Maria Madalena, state of Rio de Janeiro, Brazil (21°52′49.1″S, 41°55′0.9″W; 1167 m a.s.l.), collected by M.T.C. Thomé, F.A. Brusquetti, and T.H. Condez, from 21–28 February 2011. CFBH 27342–45, Parque Estadual do Desengano, trail to Pico do Desengano, municipality of Santa Maria Madalena, state of Rio de Janeiro, Brazil (21°52′45.3″S, 41°55′07.0″W; 1130 m a.s.l.), collected by C. Canedo, T. Brunes, M. Gehara and M.T.C. Thomé, on 20 November 2010.

Diagnosis. *Brachycephalus herculeus* **sp. nov.** is distinguished from all its congeners by the following combination of characters: (1) skin on head and dorsum with dermal ossification; (2) skull with hyperossification of postorbital crests, which can be seen externally; (3) fourth presacral vertebra with transverse processes hyperossified, not ornamented and not visible externally; (4) urostyle crest extending up to 2/3 of urostyle length; (5) long oesophageal process of hyolaryngeal apparatus; (6)

Table 1. Measurements (in millimeters) of specimens of *Brachycephalus herculeus* **sp. nov.** Abbreviations are mean ($\bar{x}$); standard deviation (SD); snout–vent length (SVL); head length (HL); head width (HW); nostril diameter (ND); internostril distance (IND); eye diameter (ED); eyelid width (EW); interorbital distance (IOD); eye–nostril distance (END); nostril–tip of snout distance (NSD); thigh length (THL); shank length (SL); foot length (FL); Toe-III length (TL); arm length (AL); forearm length (FAL); hand length (HAL); and Finger-IV length (FIL).

Measurement	Males (n = 9)			Females (n = 7)		
	$\bar{x}$	SD	Range	$\bar{x}$	SD	Range
SVL	12.4	0.8	11.8–14.7	14.4	0.5	13.9–15.2
HL	2.7	0.3	2.4–3.4	2.8	0.1	2.6–2.9
HW	5.3	0.2	5.0.–5.5	5.5	0.3	5.1–5.8
ND	0.2	0.0	0.1–0.3	0.2	0.1	0.1–0.3
IND	1.6	0.9	1.5–1.8	1.8	0.1	1.7–2.1
ED	1.5	1.0	0.8–1.2	1.6	0.1	1.6–1.8
EW	0.9	0.1	0.8–1.2	1.0	0.1	0.9–1.2
IOD	2.1	0.1	1.9–2.2	2.3	0.1	2.1–2.5
END	0.6	0.1	0.5–0.7	0.7	0.0	0.6–0.7
NSD	0.5	0.1	0.5–0.6	0.5	0.1	0.4–0.6
THL	5.0	0.6	4.1–5.9	5.9	0.3	5.5–6.4
SL	5.1	0.4	4.5–5.6	5.4	0.1	5.3–5.6
FL	7.5	0.5	6.8–8.5	8.2	0.3	7.8–8.6
TL	2.7	0.6	1.9–2.9	3.1	0.1	3.0–3.3
AL	3.9	0.4	3.2–4.5	4.4	0.5	3.8–5.0
FAL	3.4	0.5	2.9–4.6	3.6	0.2	3.2–3.9
HAL	2.5	0.4	2.1–3.5	2.6	0.2	2.2.–2.9
FIL	1.4	0.1	1.3–1.6	1.6	0.1	1.4–1.8

general color in life orange with dorsal green irregular patch; (7) presence of osteoderms; (8) presence of black connective tissue scattered over dorsal musculature; (9) medium body size for the genus (SVL of adults: 11.8–14.7 mm for males and 13.9–15.2 mm for females; (10) advertisement call characterized by one note repeated in sequence, commonly comprised of 8–12 pulses.

Comparisons with other species. The presence of hyperossification in the skeleton and skin with dermal ossification on the head and dorsum distinguish the new species from all members of the *B. pernix* species group (*B. actaeus*, *B. albolineatus*, *B. auroguttatus*, *B. boticario*, *B. brunneus*, *B. coloratus*, *B. curupira*, *B. ferruginus*, *B. fuscolineatus*, *B. izecksohni*, *B. leopardus*, *B. mariaeterezae*, *B. mirissimus*, *B. olivaceus*, *B. pernix*, *B. pombali*, *B. quiririensis*, *B. tabuleiro*, *B. tridactylus* and *B. verrucosus*; Pombal et al. 1998, 2018; Ribeiro et al. 2005, 2015, 2017; Alves et al. 2006; Garey et al. 2012; Pie et al. 2015; Bornschein et al. 2016; Monteiro et al. 2018a; Mângia et al. 2023), and from *B. clarissae*, *B. didactylus*, *B. hermogenesi*, *B. pulex*, *B. puri*, and *B. sulfuratus*, all of which lack hyperossification (Izecksohn 1971; Giaretta and Sawaya 1998; Napoli et al. 2011; Condez et al. 2016; Almeida-Silva et al. 2021; Folly et al. 2022). Also, the absence of metacarpal and metatarsal tubercles distinguishes *B. herculeus* **sp. nov.** from *B. hermogenesi* (metacarpal and metatarsal tubercles present; Giaretta and Sawaya 1998) and from *B. auroguttatus*, *B. boticario*, *B. brunneus*, *B. fuscolineatus*, *B. izecksohni*, *B. leopardus*, *B. mariaeterezae*, *B. olivaceus*, *B. pitanga*, *B. pulex*, *B. quiririensis*, *B. toby* and *B. verrucosus* (outer metatarsal tubercles present, Giaretta and Sawaya 1998; Ribeiro et al. 2005. 2015; Alves et al. 2009; Haddad et al. 2010; Napoli et al. 2011; Pie and Ribeiro 2015).

Brachycephalus herculeus **sp. nov.** lacks the quadratojugal, as in other species of the *B. ephippium* and *B. vertebralis* groups (except *B. crispus*, in which the quadratojugal may be present or not), whereas in species of the *B. pernix* group the quadratojugal is present (Ribeiro et al. 2005; Alves et al. 2006; Campos et al. 2010; Bornschein et al. 2016; Condez et al. 2016; Monteiro et al. 2018a).

The general orange background color in life of *Brachycephalus herculeus* **sp. nov.** distinguishes it from that of the flea-toads *B. didactylus*, *B. hermogenesi*, *B. pulex*, *B. puri*, and *B. sulfuratus*, which exhibit a brown or gray general body color (Izecksohn 1971; Giaretta and Sawaya 1998; Napoli et al. 2011; Condez et al. 2016; Almeida-Silva et al. 2021), and *B. clarissae*, which has the dorsal region mainly light brown and the ventral region yellow with scattered red blotches (Folly et al. 2022). The new species also has a larger body size (adult SVL: 11.8–15.2 mm; Table 1) than the aforementioned flea-toads (maximum SVL < 11 mm in all six species; Izecksohn 1971; Almeida-Santos et al. 2011; Napoli et al. 2011; Condez et al. 2016; Almeida-Silva et al. 2021; Folly et al. 2022).

Brachycephalus herculeus **sp. nov.** can be distinguished from the extremely hyperossified species of the *B. ephippium* species group (*B. darkside*, *B. ephippium*, *B. garbeanus*, *B. ibitinga*, *B. margaritatus*, and *B. rotenbergae*) by the absence of a dorsal bony shield (which is present in

Table 2. Interspecific uncorrected *p*-distances based on the 16S rRNA gene for the species within the *B. vertebralis* group. Minimum and maximum values are given as percentages (%). The number of analyzed individuals for each species (in parentheses), followed by their intraspecific distances are presented in bold.

	Species	1	2	3	4	5	6	7	8	9
1	*Brachycephalus herculeus* **sp. nov.**	**(11) 0.0**								
2	*Brachycephalus alipioi*	2.5–3.0	**(3) 0.0**							
3	*Brachycephalus bufonoides*	0.5–0.8	3.0–3.0	**(3) 0.0–0.1**						
4	*Brachycephalus crispus*	2.8–4.0	2.9–3.5	4.2–5.1	**(2) 0.1**					
5	*Brachycephalus guarani*	3.2–4.9	2.1–3.1	4.1–5.1	0.3–1.3	**(3) 0.0–0.1**				
6	*Brachycephalus nodoterga*	3.0–4.3	2.0–2.8	4.0–4.6	1.7–2.7	1.8–2.9	**(6) 0.0–0.1**			
7	*Brachycephalus pitanga*	2.8–4.0	2.2–2.4	4.0–4.2	0.0–0.1	0.1	1.6–2.1	**(2) 0.0**		
8	*Brachycephalus toby*	3.2–4.3	1.9–2.4	3.9–4.1	1.5–2.3	1.6–1.8	0.3–0.7	1.5–1.7	**(3) 0.0**	
9	*Brachycephalus vertebralis*	2.8–3.8	1.9–2.5	3.6–4.0	0.1–1.4	0.1–1.3	1.3–2.1	0.6–0.8	1.2–1.3	**(4) 0.0**

those species; Pombal 2010; Pombal and Izecksohn 2011; Guimarães et al. 2017; Nunes et al 2021; Condez et al. 2021). Further, *Brachycephalus herculeus* **sp. nov.** exhibits black connective tissue scattered over the dorsal musculature (Fig. 2). This feature distinguishes this species from *B. izecksohni*, *B. pernix*, and *B. pitanga*, all of which lack this pigmentation (Guimarães et al. 2017). Regarding *B. garbeanus* and *B. margaritatus*, some specimens of these species were reported to present a few scattered areas with dark pigmentation in the dorsolateral region adjacent to the dorsal musculature, while in *B. vertebralis* there is some internal dark pigmentation around the vertebral column (Guimarães et al. 2017).

The new species is easily separated from other species of the *B. vertebralis* species group, except *B. toby*, by its general color orange with a green irregular patch on the dorsum (see color pictures of other species of the *B. vertebralis* group in Pombal and Gasparini 2006; Alves et al. 2009; Haddad et al. 2013; Condez et al. 2014; Clemente-Carvalho et al. 2016; Folly et al. 2020). Also, *B. herculeus* **sp. nov.** can be separated from the other species of the *B. vertebralis* group, except for *B. nodoterga* and *B. crispus*, by the presence of wart-like osteoderms on the skin of the dorsum, flanks, venter, arms, and legs (see Folly et al. 2021a). The new species' dorsal aspect is similar to that of *B. nodoterga*, which also presents greenish coloration on dorsal surfaces, but differs from the latter in that its dorsal color is leaf green (olive green in *B. nodoterga*) and does not extend to the flanks and to the sides of the head as it does in *B. nodoterga*.

Brachycephalus herculeus **sp. nov.** is the sister species of *B. bufonoides* according to our molecular analysis (Fig. 3). These species exhibit some of the smallest interspecific genetic distances among all pairs of species within the *Brachycephalus vertebralis* group (Table 2). They also share a prominent pelvic region, which is externally marked as a v-shaped bulge (presumably representing the protrusion of the iliac bones underneath) whose vertex lies at the posterior end of the body and whose tips extend to the middle of the trunk on either side; this characteristic distinguishes *Brachycephalus herculeus* **sp. nov.** and *B. bufonoides* from the other species of the *B. vertebralis* group. Notwithstanding, *Brachycephalus herculeus* **sp. nov.** is easily distinguished from *B. bufonoides* by the presence of osteoderms on the skin (absent in *B. bufonoides*), by its greenish dorsal color in life (orange in *B. bufonoides*), and by the advertisement call comprised by notes with 10–12 pulses (notes with 13–17 pulses in *B. bufonoides*). Furthermore, in terms of osteology and internal anatomy, the new species can be also distinguished from *B. bufonoides* by its lateroposteriorly oriented parotic plate (posteriorly oriented in *B. bufonoides*), oesophageal process of hyolaryngeal cartilages longer than arytaenoids (shorter than arytenoids in *B. bufonoides*), absence of an elbow sesamoid (present in *B. bufonoides*), paravertebral plates not ornamented (ornamented in *B. bufonoides*), and dorsal crest of the urostyle extending for 2/3 of its length (extending for all its length in *B. bufonoides*; Folly et al. 2020, 2021a).

Description of the holotype. Adult male; head wider than long (HL/HW = 0.42%); head length approximately 18% of SVL; snout short, with length equivalent to 77% of eye diameter, rounded in lateral and dorsal views; nostrils protuberant, oriented posterolaterally; canthus rostralis distinct and straight; loreal region weakly concave; mouth nearly sigmoid; eye slightly protruding in dorsal and lateral views, eye diameter 60% of HL; tympanum absent; choanae relatively small and round; vomerine odontophores absent. Upper arm around 78% of forearm length; length of upper arm plus forearm 58% of SVL; hand 58% of upper-arm length; fingers III and IV distinct; fingers II and V vestigial; tip of finger III rounded, tip

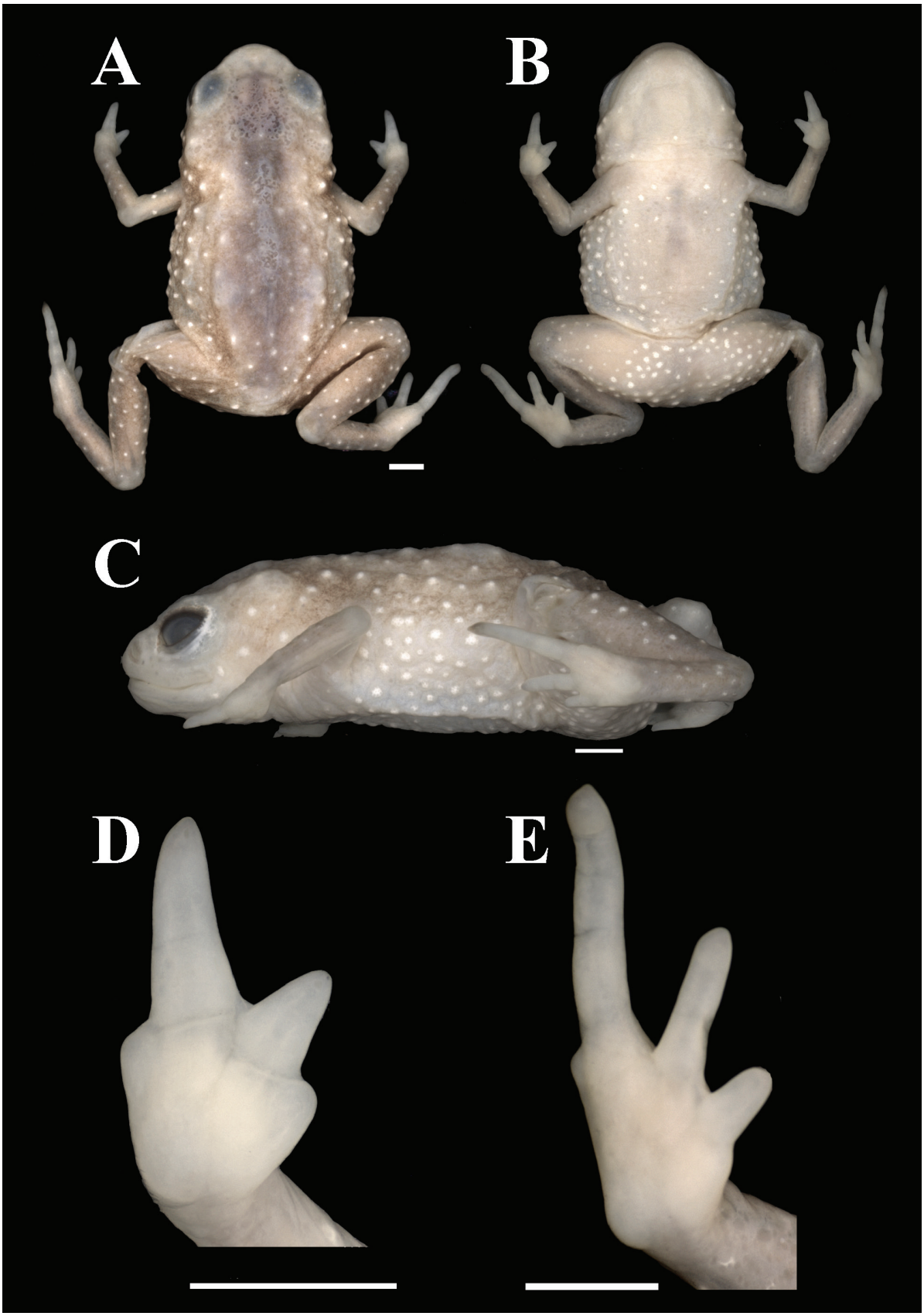

Figure 1. Holotype of *herculeus*, new species (MNRJ 42408). **A** Dorsal, **B** ventral, and **C** lateral views of the body; **D** ventral view of foot, and **E** ventral view of hand. Scale bar = 1 mm.

of finger IV slightly pointed; finger III smaller than finger IV; metacarpal tubercles absent. Tibia slightly shorter than thigh (TL/THL = 0.90); thigh and tibia 86% of SVL; foot longer than thigh (FL/THL = 0.76); toe I externally absent and toe V vestigial; toes II, III, and IV distinct; toe II reduced; tip of toes II and III rounded, tip of Toe-IV

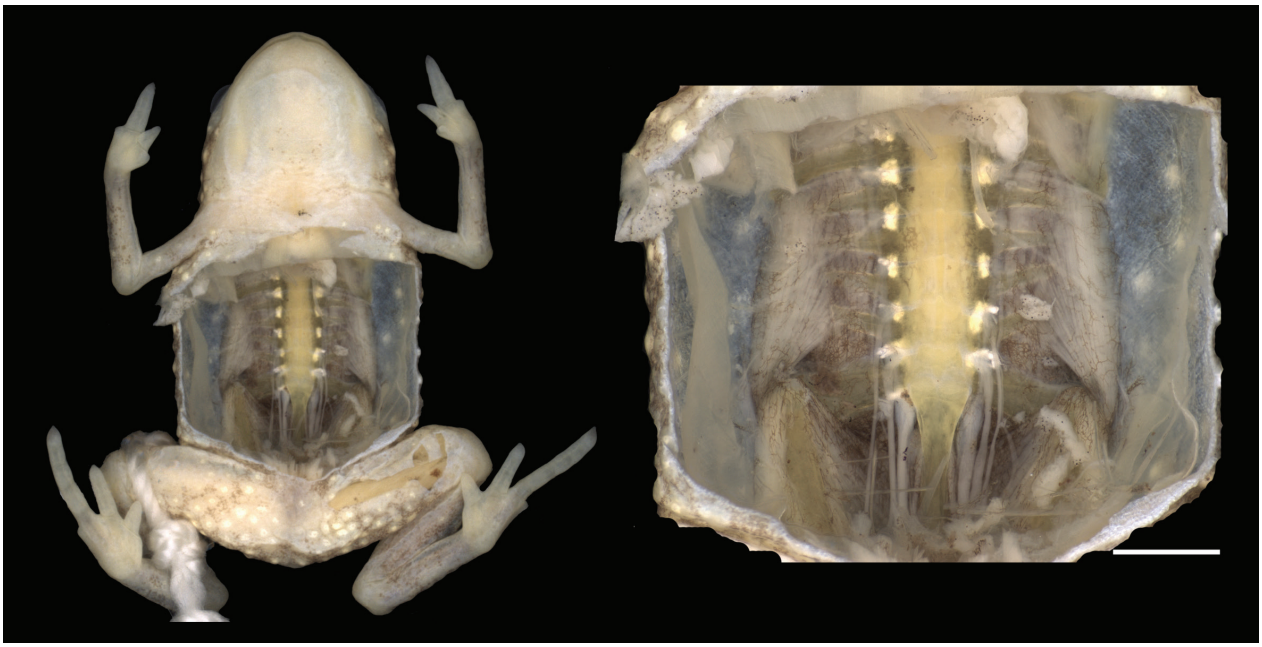

Figure 2. Ventral and dorsal view of dissected preserved specimens of *Brachycephalus herculeus*, new species (CFBH 28130), showing scattered areas with pigmentation (dark tissue) in the dorsolateral region adjacent to the dorsal musculature, also around the line of the spinal vertebrae.

pointed; relative length of toes II < III < IV; metatarsal tubercles absent. Skin on dorsum, flanks, venter, and dorsal and ventral surface of legs and forearms with warty appearance, due to the presence of osteoderms; granular skin on ventrolateral surfaces of body and area around the cloacal opening.

Measurements of holotype (in mm). SVL 13.4; HL 2.5; HW 6.0; ND 0.1; IND 1.7; ED 1.5; EW 1.1; IOD 2.2; END 0.7; NSD 0.4; THL 6.1; SL 5.5; FL 8.1; TL 2.8; AL 4.4; FAL 3.4; HAL 2.5; FIL 1.3.

Coloration of holotype in preservative (Fig. 1). Forearms and legs gray; hands, feet, arms, lateral and ventral sides of the body beige; two contiguous dorsal paired dark gray marks bordering the vertebral column; scattered whitish warts (osteoderms) on the dorsum, flanks, arms, and legs; a cream line below each eye.

Color in life (Fig. 4). General background color orange; central area of head and dorsum and dorsal part of thighs and shanks green. Osteoderms, appearing as light yellow "warts" distributed throughout most of the body and limbs. Hands, feet, elbows, knees, and ankles orange. Ventral surface of body bright yellow. Eyes entirely black, with no visible delimitation between pupil and iris.

Variation. Morphometric variation is given in Table 1. On average, females (SVL = 14.5 ± 0.4 mm; 13.9–15.2 mm, n = 9) of *B. herculeus* are larger (Welch's t-test, t = 4.6443, df = 15.579, p < 0.0003) than males (SVL = 12.8 ± 1.1 mm; 11.8–14.7 mm, n = 11). Semicircular or rounded snout in dorsal view and rounded in lateral view. The density of osteoderms in the skin may vary among individuals, but osteoderms are always less numerous on the mid-dorsal and mid-ventral regions and practically absent on the dorsum of head and gular region (Figs 4–6). Spinal plates weakly to well-delimited externally (Fig. 5). In preservative, dorsal and lateral surfaces of body can be cream to gray, varying especially on the head and limbs. A dissected preserved specimen (CFBH 28130), show scattered areas with pigmentation (dark tissue) in the dorsolateral region adjacent to the dorsal musculature, also around the line of the spinal vertebrae (Fig. 2). The visibility of black connective tissue scattered over the dorsal musculature is externally represented, in most specimens (70% of the type-series), by paired contiguous dorsal dark gray marks bordering the vertebral column (Fig. 5).

Distribution (Fig. 7). *Brachycephalus herculeus* **sp. nov.**, is known only from the type-locality, the Parque Estadual do Desengano, in the municipality of Santa Maria Madalena, state of Rio de Janeiro, southeastern Brazil. This site is located within the northern portion of the Serra do Mar Mountain Range.

Natural history. The new species lives amidst the leaf-litter and can be found active during the day. Most individuals were found hidden amidst the leaf-litter, under fallen trunks, and among roots. The holotype and paratype (MNRJ 42407) were collected on the ground, during nocturnal surveys. The holotype was collected using quadrat sampling (see Siqueira et al. 2011) and thus may have been disturbed by the revolving of the leaf litter during the survey, so it is uncertain if it was active at night. The latter specimen may also have been found inactive under a decomposing leaf at the time. Paratype (MNRJ 42409) was found during the afternoon (at 1500 h) inside a bromeliad (*Vriesea* sp.) that was attached to a tree stump, ca. 80 cm from the ground. The specimens collected in 2011,

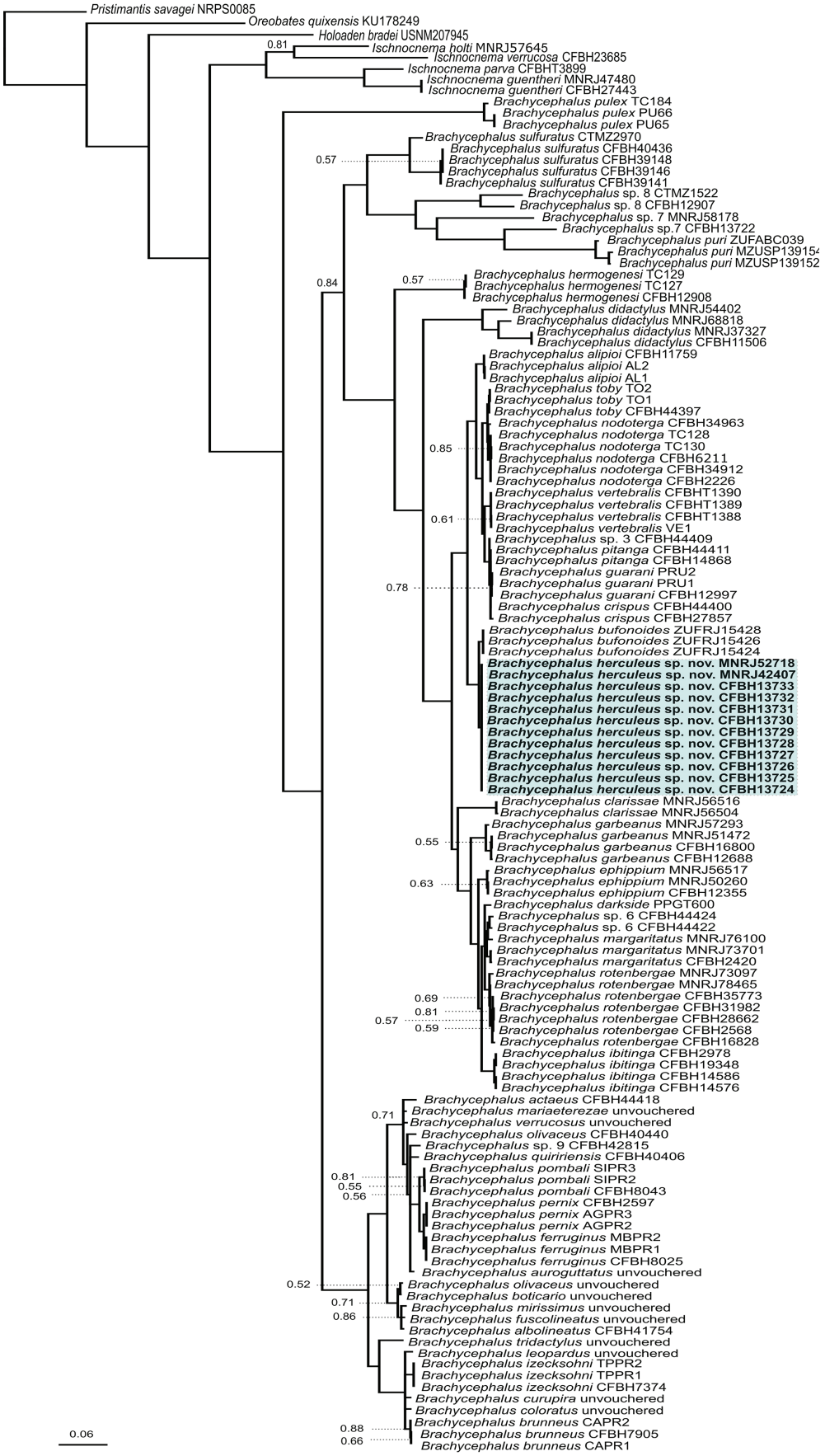

Figure 3. The majority rule consensus tree resulting from the Bayesian Inference analysis based on the concatenated alignment of 5456 bp (four mitochondrial and three nuclear genes) showing the relationships within *Brachycephalus*. Sequences of the new species are highlighted in blue. Numbers associated to nodes represent Bayesian Posterior Probabilities < 0.90; all other nodes were fully supported (BPP = 1.0). Voucher numbers of specimens are provided at each terminal, when available. See Table S2 for the GenBank accession numbers.

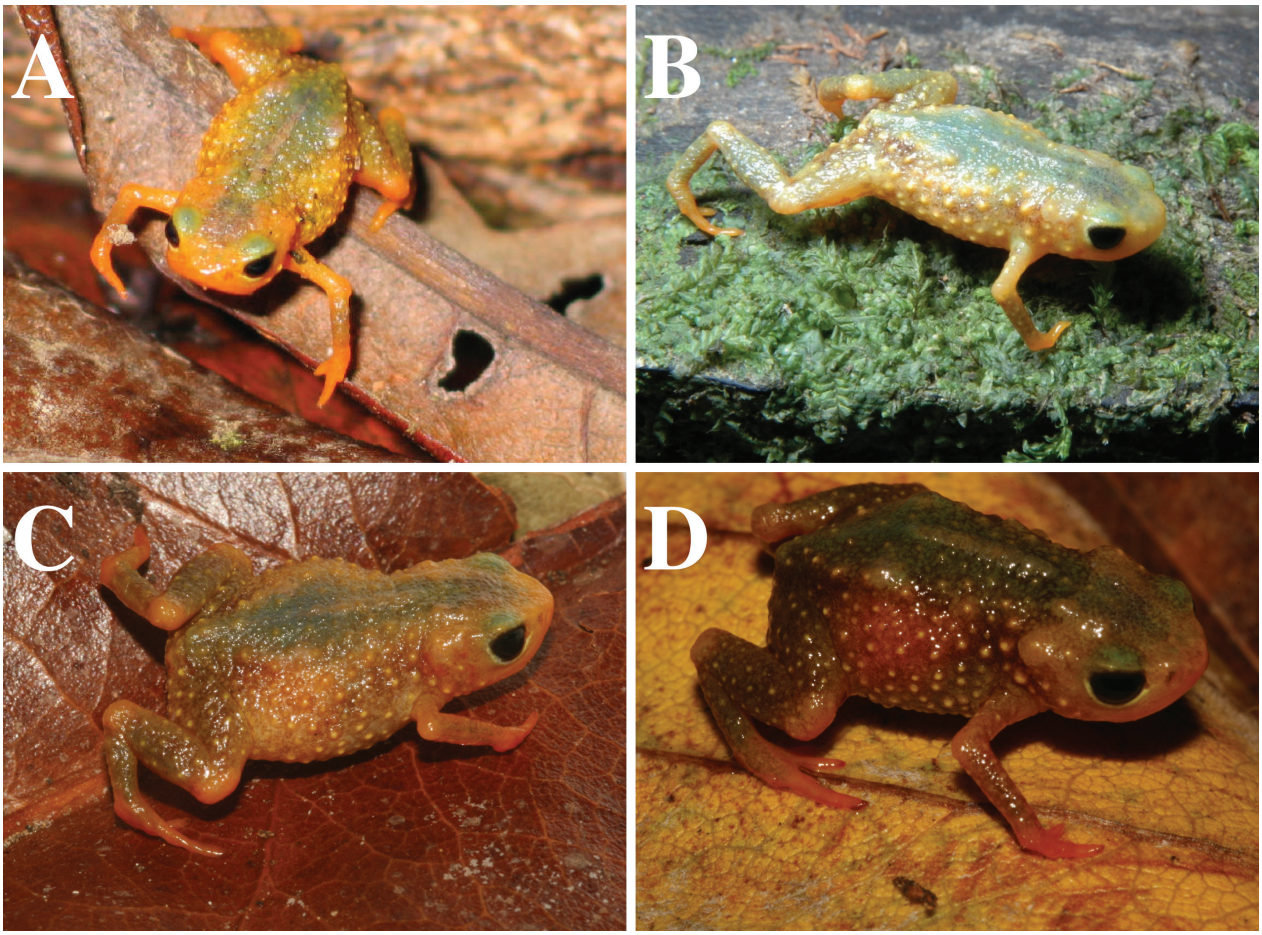

Figure 4. Four specimens of *Brachycephalus herculeus*, new species, in life. Photographs by C. F. D. Rocha (**A**), C. F. B. Haddad (**B**) and T. H. Condez (**C**, **D**).

during the rainy season, were on sloping terrain bordering trails in the forest. Males were not observed exposed when calling. An amplectant pair was found hidden under the leaf-litter in February 2011, during the morning after a rainy night. When exposed, the male changed its axillary amplexus to inguinal, as described for *B. rotenbergae* (Pombal et al., 1994, where it was called *B. ephippium*) and the pair moved away looking for shelter. Minutes after having hidden among the leaf litter, the female left the place and the male remained immobile. No eggs were found.

Advertisement call (Fig. 8). The advertisement call of the new species is characterized by one pulsed note repeated in sequence, at a rate of 2.5–2.7 notes/s (2.6 ± 0.08 s; n = 60; Fig. 8). Call repetition may last for minutes and suggests a long period of calling activity. The call (or note) has a duration of 0.21–0.33 s (0.25 ± 0.05 s; n = 60) and the inter-call (or inter-note) interval is 0.19–0.20 s (0.19 ± 0.00 s; n = 80) long. Notes are comprised of 10–12 pulses (11.0 ± 1.0; n = 60), with each pulse lasting 0.02 ± 0.00 s (n = 60), and the pulse repetition rate is 27–31 pulses/s (29.0 ± 1.70 pulses/s; n = 60). The lower frequency range is 3.7–4.3 kHz (3.9 ± 0.26 kHz; n = 60), that of the upper frequency is 6.0–6.4 kHz (6.2 ± 0.17 kHz; n = 60), and that of the dominant frequency is 4.5–5.1 kHz (4.8 ± 0.24 kHz; n = 60).

The main structure of the advertisement call of the new species, characterized by one note repeated in sequence, commonly comprised of 10–12 pulses, distinguishes it from the advertisement call of *B. actaeus*, *B. albolineatus*, *B. hermogenesi*, *B. mirissimus*, *B. olivaceus*, *B. pernix*, *B. quiririensis*, *B. tridactylus* (in which the notes are comprised of 1–4 pulses; Monteiro et al. 2018a,b; Bornschein et al. 2018; Pie et al. 2018; Bornschein et al. 2019), *B. sulfuratus* (notes comprised of 4–7 pulses; Condez et al. 2016), and *B. darkside* (notes comprised of 6–8 pulses; Guimarães et al. 2017). Additionally, the dominant frequency of the advertisement call in the new species, ranging from 4.5–5.1 kHz (average of 4.8 ± 0.24 kHz) is also distinct from the ones described for *B. hermogenesi* (average of 6.8 ± 0.24 kHz; Verdade et al. 2008), *B. sulfuratus* (6.2–7.2 kHz, average of 6.7 ± 0.3 kHz; Condez et al. 2016), *B. olivaceus* (6.4–7.0 kHz, average of 6.2 ± 0.2 kHz; Monteiro et al. 2018b), *B. quiririensis* (6.2–6.5 kHz, average of 6.3 ± 0.2 kHz; Monteiro et al. 2018b), *B. actaeus* (6.6–7.3 kHz, average of 6.9 ± 0.3 kHz; Monteiro et al. 2018a), *B. rotenbergae* (2.8–4.5 kHz, average of 3.8 ± 0.35 kHz; Nunes et al. 2021), and *B. darkside* (2.9–3.8 kHz, average of 3.4 ± 1.8; Guimarães et al. 2017). The call duration in the new species (0.21–0.33 s, average of 0.25 ± 0.05 s) differs from that of *B. darkside* (0.08–0.16 s, average of 0.11 ± 0.13 s; Guimarães et al. 2017). Some temporal and spectral parameters of

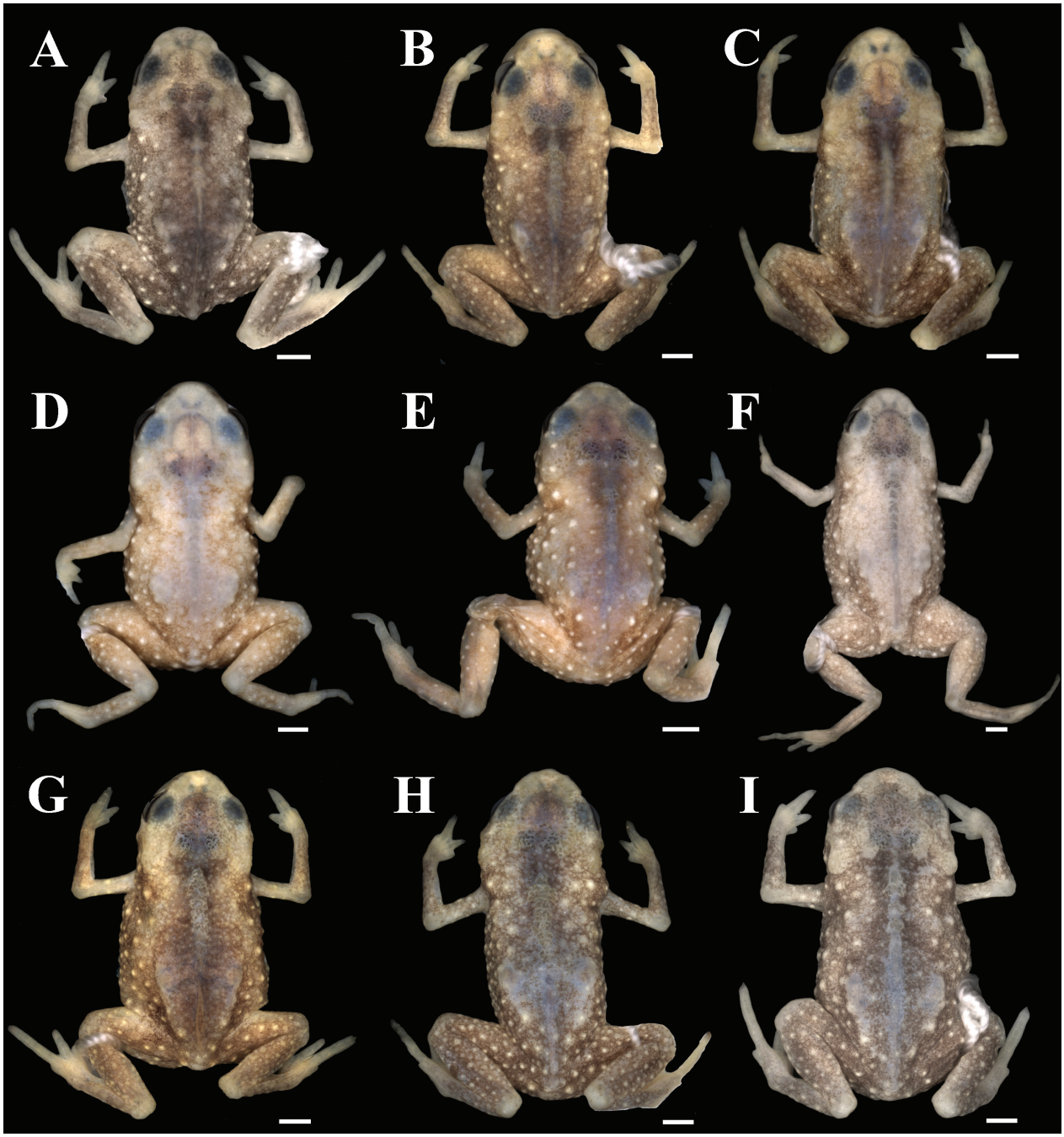

Figure 5. Dorsal variation in preserved specimens of *Brachycephalus herculeus*, new species. **A** CFBH 28124 (male; SVL 12.0 mm), **B** CFBH 28129 (male; SVL 12.2 mm), **C** CFBH 28135 (male; SVL 12.3 mm), **D** MNRJ 52721 (male; SVL 11.8 mm), **E** MNRJ 42409 (male; SVL 12.0 mm), **F** MNRJ 52718 (female; SVL 15.2 mm), **G** CFBH 28132 (female; SVL 14.1 mm), **H** CFBH 28136 (female; SVL 15.1 mm), and **I** CFBH 28138 (female; SVL 14.4 mm). Scale bar = 1 mm.

the advertisement call of *Brachycephalus herculeus* **sp. nov.** overlap with those described for *B. crispus*, *B. pitanga*, *B. bufonoides*, and *B. ibitinga* (Condez et al. 2014; Oliveira and Haddad 2017; Folly et al. 2020; Condez et al. 2021). Among these species, the number of pulses per call (10–12 pulses) distinguishes the new species from *B. bufonoides* (notes comprised of 13–17 pulses; Folly et al. 2020). The inter-call (or inter-note) interval for the new species (0.19–0.20 s) differs from the ones described for *B. crispus* (average of 0.35 s; Condez et al. 2014), *B. pitanga* (average of 0.27 s; Oliveira and Haddad 2017), and *B. ibitinga* (0.28–0.37 s, average of 0.32 s; Condez et al. 2021). The note repetition rate (2.5–2.7 notes/s, average of 2.6 notes/s) reported for the new species differs from those of *B. crispus* (average of 1.7 notes/s; Condez et al. 2014), *B. bufonoides* (2.0–2.4 notes/s; Folly et al. 2020), and *B. ibitinga* (average of 1.8 notes/s; Condez et al. 2021).

Etymology. Herculeus is a Latin adjective meaning very great, difficult, or dangerous; requiring the strength or courage of Hercules to challenge or accomplish a mission, as herculean labor or task (derived from Greek Mythology). The specific epithet was chosen to represent the

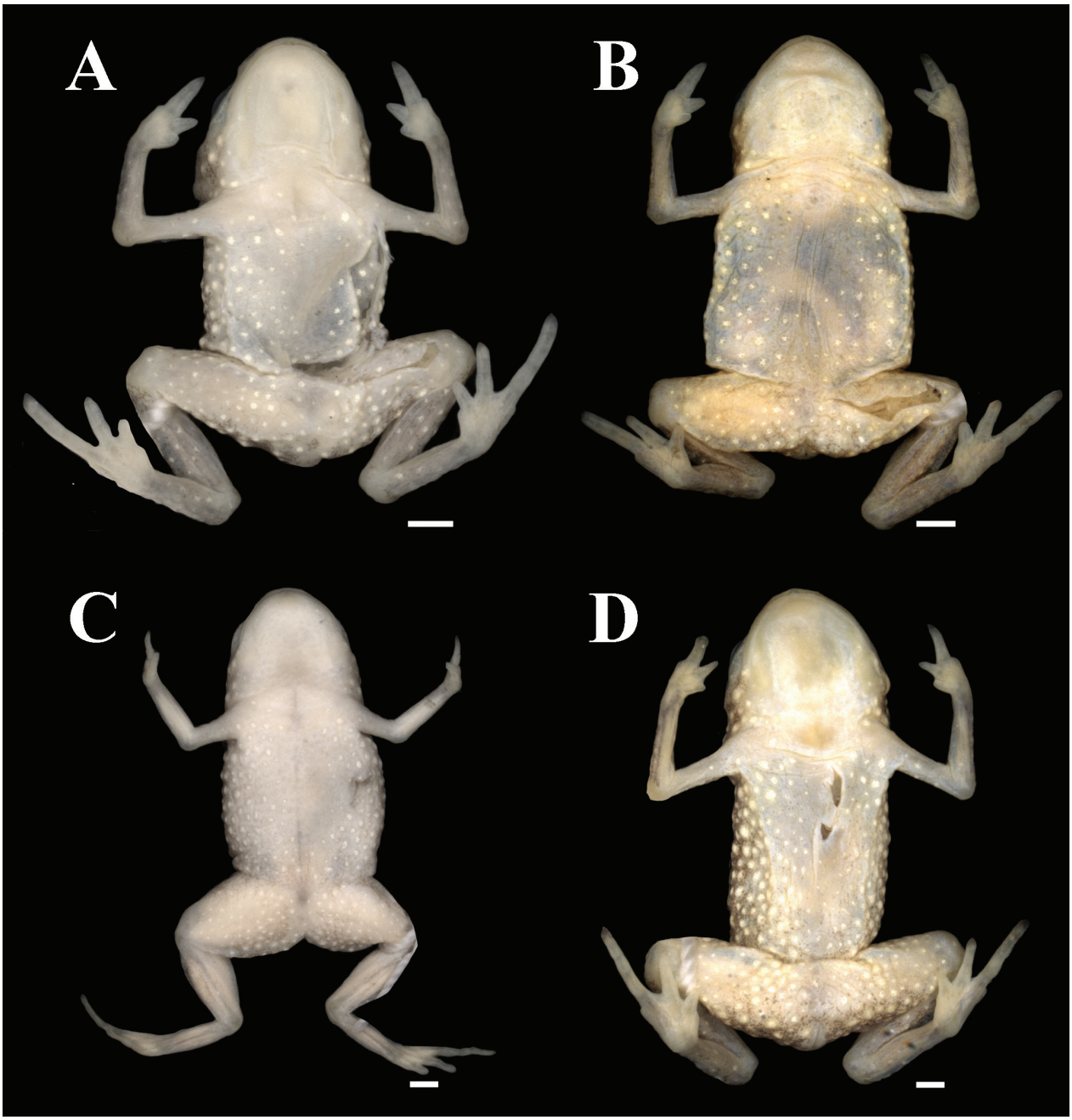

Figure 6. Ventral variation in preserved specimens of *Brachycephalus herculeus*, new species. **A** CFBH 28124 (male; SVL 12.0 mm), **B** CFBH 28132 (female; SVL 14.1 mm), **C** MNRJ 52718 (female; SVL 15.2 mm), and **D** CFBH 28136 (female; SVL 15.1 mm). Scale bar = 1 mm.

"herculean" task that is, for such a small species, to survive in one of the most threatened forest environments in the world, the Brazilian Atlantic Forest.

Molecular analysis. We obtained a final aligned matrix of 5,456 base pairs considering the selected mitochondrial and nuclear gene fragments. The optimal partition scheme and nucleotide substitution models selected for each data block were GTR+I+G (12S rRNA, 16S rRNA), K80+G (fist codon position of COI), GTR+I (second codon positions of COI and cyt *b*), GTR+G (three codon positions of Tyr; first codon positions of RAG1 and RAG2; third positions of COI and cyt *b*), SYM+I+G (first codon position of cyt *b*), HKY (second codon positions of RAG1 and RAG2), HKY+G (third codon position of RAG1), K80+I (third codon position of RAG2). Our main results corroborate many of the previously published phylogenetic hypotheses for the genus *Brachycephalus* but differs from those with respect to the position of the flea-toads *B. clarissae*, *B. hermogenesi*, *B. puri*, *B. sulfuratus*, and the candidate species *B.* sp. 7 and *B.* sp. 8 (Fig. 3). Nevertheless, our hypothesis supports the position of *B. pulex* as sister to all other *Brachycephalus* species, as suggested in previous studies (Almeida-Silva et al. 2021; Dos Reis et al. 2021; Lyra et al. 2021). It also corroborates the position of *B. didactylus* as the sister species of the clade comprised of the *B. ephippium* and *B. vertebralis* species groups (Condez et al. 2020; Dos Reis et al. 2021; Almei-

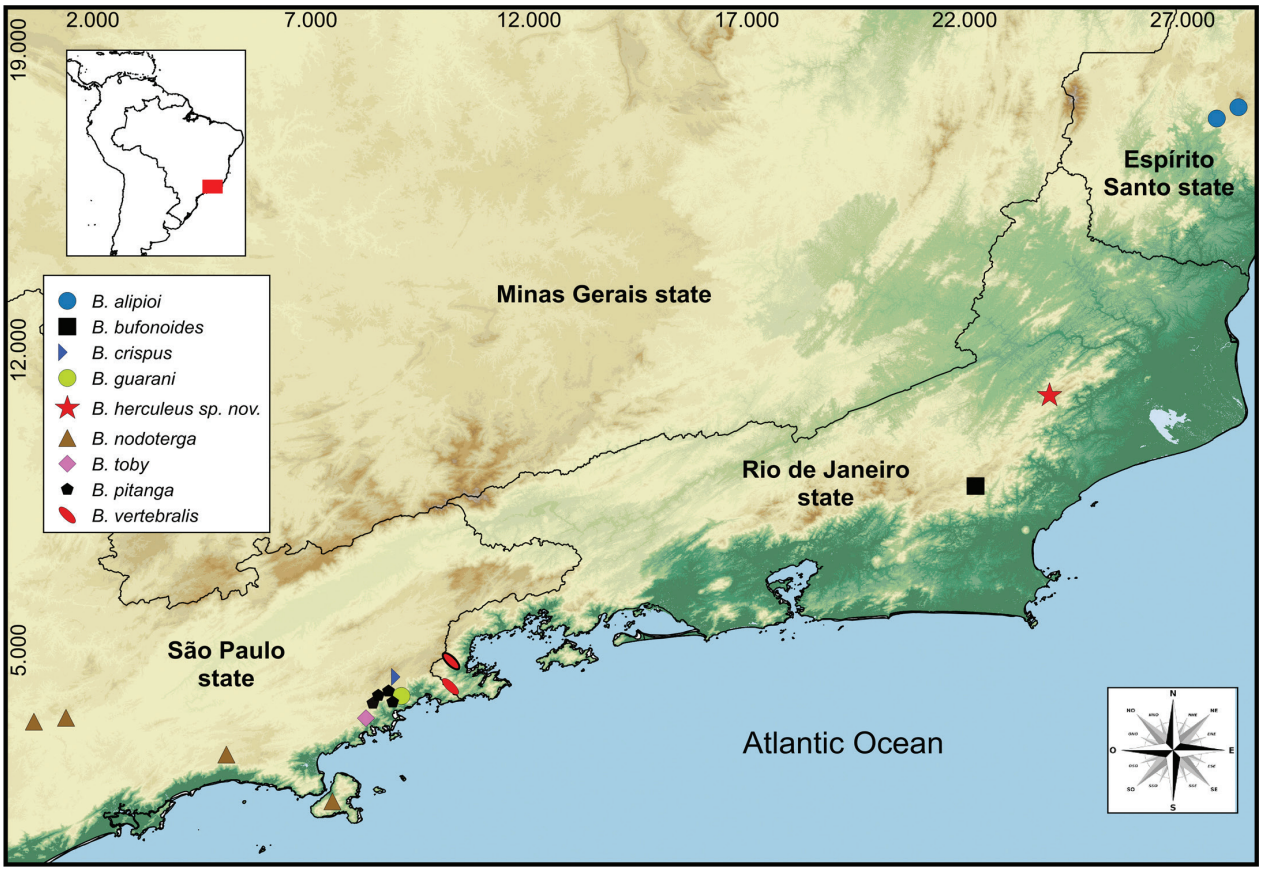

Figure 7. Geographic distribution of the hyperossified species within the *Brachycephalus vertebralis* species group. Note the occurrence of *Brachycephalus herculeus*, new species, in the state of Rio de Janeiro, southeastern Brazil.

da-Silva et al. 2021; Folly et al. 2022). However, our analysis diverges from previous studies in the phylogenetic positions of *B. hermogenesi*, which is known to be fairly controversial in the literature (see Lyra et al. 2021), and of *B. clarissae* (sister to the *B. ephippium* group instead of the *B. vertebralis* group (as *B. vertebralis* lineage) as in Condez et al. 2020 or the *B. ephippium* + *B. vertebralis* groups as in Folly et al. 2022). *Brachycephalus sulfuratus* was recovered as the sister species to a clade containing *B. puri* and two undescribed taxa (*Brachycephalus* sp. 7 and *Brachycephalus* sp. 8), but its position relative to the pumpkin-toadlets remains unstable (e.g., Condez et al. 2020; Folly et al. 2020, 2022; Lyra et al. 2021). The position of *B. puri* in our tree was distinct from that presented at the original description of the species (Almeida-Silva et al. 2021), probably due to the inclusion of samples of the two flea-toad candidate species in our dataset. *Brachycephalus herculeus*, new species, was recovered as monophyletic in our phylogenetic reconstruction, and was nested within the *B. vertebralis* species group, as the sister species of *B. bufonoides* (Fig. 3). Based on the genetic distances for the 16S rRNA gene (1548 bp), the sequences of different individuals of the new species did not differ from each other (*p*-distance = 0; n = 11). Within the *B. vertebralis* species group, the smallest genetic divergences between the new species and other congeners were 0.5–0.8% (from its sister species *B. bufonoides*) and the greatest was 4.9% (from *B. guarani*; Table 2).

Osteological description. ***Skull*** (Figs 9, 10). Shape and proportions: Isolated bony structures (osteoderms) are predominantly distributed on the lateral surfaces of the body. The skull is wider than long (length/width range 85–95%). The diameter of the orbit is 39–47% of the total length of the skull. The skull is widest at the prootics, and the jaw articulation lies anterior to the posterior end of the skull at the occipital condyles. The upper jaws are relatively short, with the posterior apex lying at the level of the optic fenestra. Large additional elements associated with the skull (parotic plate) and vertebrae (vertebral and paravertebral plates) are dermal bones. — ***Skull plate.*** Exostosis and co-ossification are present in the skull forming an ornamented ridge-like pattern. Thus, nasals, dermal sphenethmoid, frontoparietals, squamosals, and the parotic plate are synostosed and exostosed, forming a dorsal skull plate. A marginal extension of the frontoparietals is fused to the parotic plate, dorsally covering the exoccipitals and prootics. There is a space between the parotic plate and a post-orbital crest forming a small concavity that reaches half of the width of the orbit. The parotic plate is connected and fused medially to the frontoparietal and has a lateroposterior orientation related to the main axis of the skull. The anterior extension of the parotic plate is small, not covering the articulation between squamosal and prootic and the posterior extension does not reach the posterior border of the occipital condyle. The post-orbital crest is latero-posteriorly projected and well developed, reaching the height of occipital con-

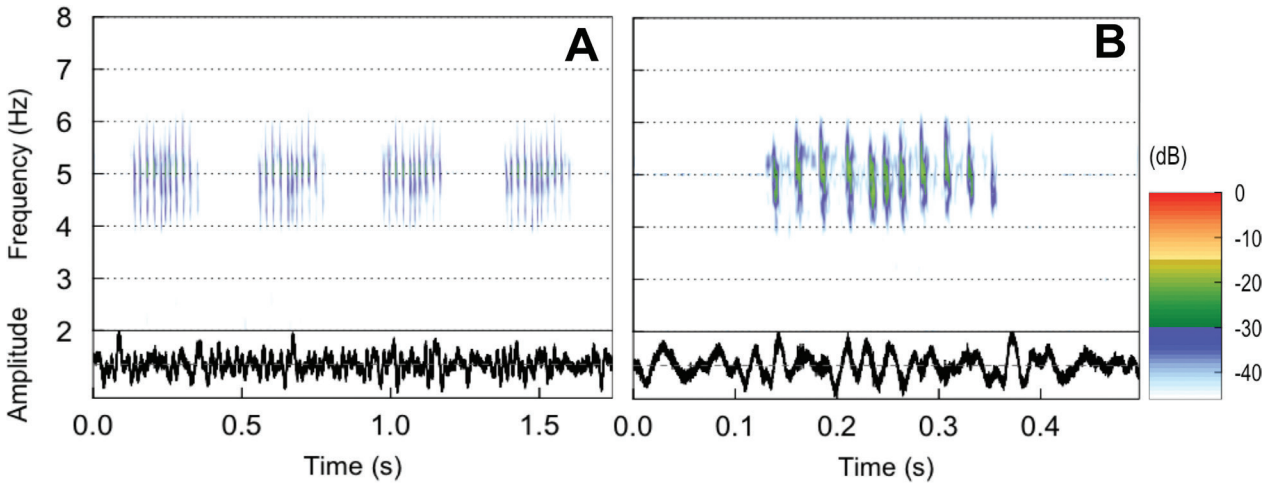

Figure 8. Advertisement call of *Brachycephalus herculeus*, new species (FNJV 58774), recorded at Parque Estadual do Desengano, municipality of Santa Maria Madalena, state of Rio de Janeiro, Brazil, 23 February 2011, at 16:00 p.m., air temperature 20.1°C, relative air humidity 88%. **A** Spectrogram (above) and oscillogram (low quality; below) of four consecutive calls (or notes), **B** Spectrogram (above) and oscillogram (low quality; below) of one pulsed call (or note).

dyle. — ***Dermal investing bones.*** Nasals: Exostosed. These bones are completely synostosed with the sphenethmoid but are not in anteromedial contact. An attenuate maxillary process contacts the preorbital process of the pars facialis of the maxilla. Frontoparietals: Expanded and exostosed. — ***Neurocranium.*** Sphenethmoid: Expanded. This bone is dorsally covered by frontoparietals and nasals. The cartilaginous optic fenestrae are absent. Fused Exoccipitals and Prootics: Not expanded and nor exostosed. The epiotic eminence (anterior and posterior) is undetectable. These bones are dorsally covered by the skull plate (frontoparietal fused with parotic plate). — ***Ventral investing bones.*** Parasphenoid: The cultriform process is synostosed with the sphenethmoid (Fig. 9). The parasphenoid alae are broad and laterally oriented beneath the otic capsule; the distal margins of the alae are wider than the proximal margins, terminating between the first third and the midpoint of the otic capsule. The posterior margin (posteromedial process) of the parasphenoid terminates in a triangular apex that lye the foramen magnum. Neopalatine: Absent. Vomers: Reduced. The anterior process is triangular with a rounded tip and is around the same length of the prechoanal process. The reduced prechoanal process forms the anterior and anteromedial margins of the choana and terminates in a rounded tip. The postchoanal process forms the posteromedial margin of the choana. The posteromedial margins of the vomers are moderately separated from each other, diverging abruptly anteriorly. The pre and postchoanal processes are around the same length. The dentigerous process is absent. — ***Maxillary arcade.*** Premaxillae: Each premaxilla is broad and separated from each other by a short gap in anterior view. The pars dentalis of each premaxilla lack teeth. In anterior view, the height of the alary process corresponds to around the length of premaxillae, and the distal tip of each alary process is pointed. The basal parts of the alary processes converge medially. The distal tips diverge from one another. Laterally, the alary processes are curved. The distal end of each pars palatina is sharp and converges to each other almost touching one another. Maxillae: The anterior end of the maxilla overlaps the posterolateral end of the premaxilla. Maxilla toothless; its posterior end is rounded and does not reach the ventral ramus of the squamosal. The pars facialis is high and thin, extending for less than half the length of the maxilla. Quadratojugals: Absent. — ***Suspensory apparatus.*** Pterygoids: The anterior ramus of each pterygoid is long, cylindrical, terminating in a truncated apex and extending to the final third of the maxilla. The medial ramus is short, slightly laminar, has a truncated end, and invests the prootic. The posterior ramus is long, triangular, and has a truncated point. Squamosals: Expanded and exostosed. They are composed of three rami that render each squamosal as a "T" shaped element composed by the ventral ramus, the otic ramus (posterior ramus), and the zygomatic ramus (anterior ramus). The ventral ramus is the longest of the three and has a rounded distal end, which is wider than its proximal portion. In lateral view, the zygomatic ramus is reduced, shorter than the ventral ramus and the distal end is rounded towards the maxilla, but without contacting it. In lateral view, the otic ramus is longer than the zygomatic ramus, and its distal end is rounded. In dorsal view, the distal end of the otic ramus is truncated, towards the parotic plate, overlapping it. Mandible: The mentomeckelian bones are in the anterior part of the mandible and are separated from each other by a short space. In anterior view, the mentomeckelians are sharp anteriorly and are fused to the dentaries laterally. Each dentary invests laterally less than half of the angulosplenial bone and has a pointed posterior end. They do not overlap the Meckel's cartilage anterolaterally. The anterior end of each angulosplenial is roundly pointed, and the posterior end is robust and rounded. The posterior end of the angulosplenial bears a well-developed pars articularis process. — ***Auditory Apparatus.*** Columellae absent. Fenestra ovalis posteriorly oriented. An enlarged and completely ossified operculum nearly fills the fenestra ovalis. — ***Hyolaryngeal skeleton***

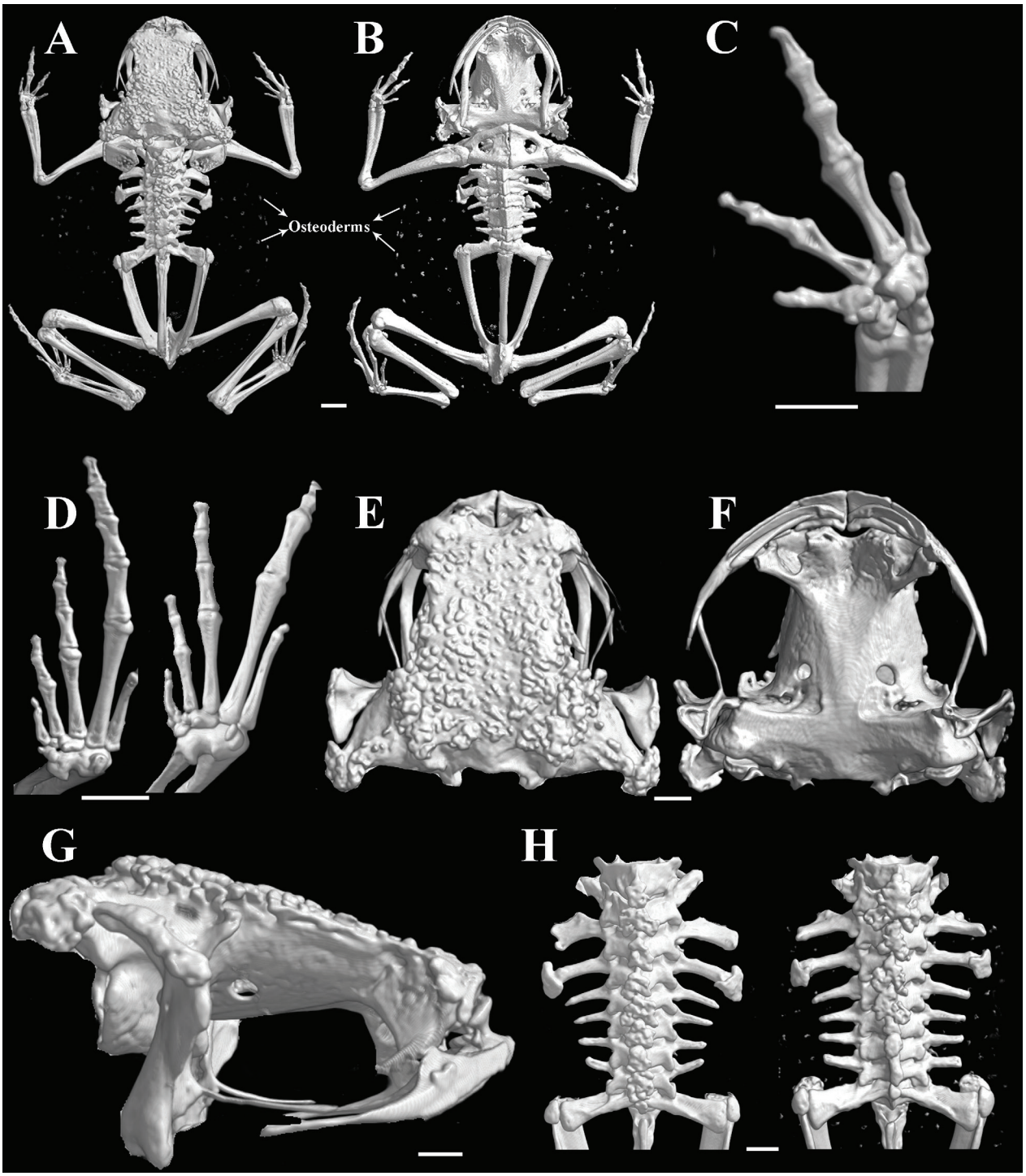

Figure 9. High-resolution computed tomography (Micro-CT) scans of paratypes of *Brachycephalus herculeus*, new species, showing osteological features. **A** Dorsal, **B** ventral views of the skeleton (CFBH 28131); **C** left hand in palmar view (CFBH 28133); **D** right foot in plantar view (CFBH 28048 and 28137, respectively); **E** dorsal, **F** ventral, and **G** lateral views of the skull (without the lower jaw; CFBH 28133); **H** dorsal view of vertebral column (CFBH 28137 and 28133, respectively). The dots surround the skeleton in (**A**) and (**B**) are osteoderms. Scale bars = 1 mm.

(Fig. 10)**.** The hyoid plate is longer than wide, with its length around four times its smallest width. The anterior processes are long and form a deep hyoglossal sinus, which deepens to nearly the height of the alary processes. The alary and posterolateral processes are much reduced, and the former is longer than the posterolateral processes. The posteromedial processes diverge widely to embrace the broad larynx. The arytenoids are short, semicircular and narrowly separated from each other, while the oesophageal process is longer than the arytenoids. — ***Postcranium*** (Fig. 9)**.** Pectoral girdle: The clavicle, procoracoid, epicoracoid, coracoid, and scapula are completely ossified and fused, with a large fenestra separating the clavicle from coracoid; suprascapula not expanded, with anterior half ossified as cleithrum; omosternum and sternum absent. The two sides of the coracoid are well-devel-

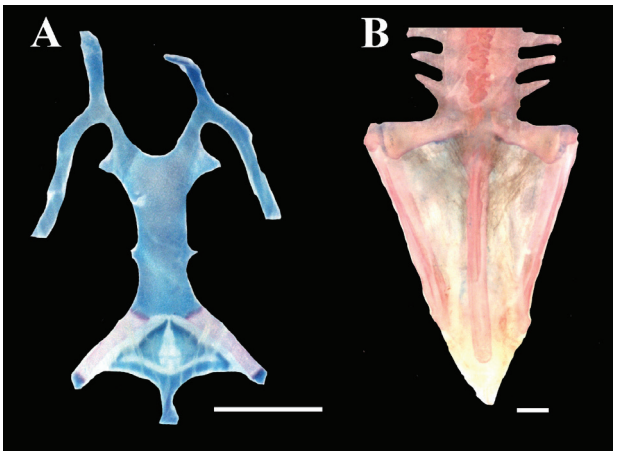

Figure 10. Views of (**A**) hyolaryngeal skeleton and (**B**) pelvic girdle of one of the paratypes of *Brachycephalus herculeus*, new species (MNRJ 42407).
Scale bar = 1 mm.

oped with a concave-shaped coracoid and around the same height giving a quadrangular appearance to the scapular apparatus. The distal edge of the clavicle bears a dorsal projection. Vertebral column: The vertebral column is composed of eight presacral, non-imbricate vertebrae. Transverse processes of Presacrals III, VI and VII are perpendicular to the notochordal axis, those of Presacrals IV and V are inclined posteriorly, and those of Presacrals II and VIII are inclined anteriorly. Relative lengths of the transverse process of presacrals IV > SD > III > V–VIII > II > I. Sacral diapophyses (SD) are moderately expanded and slightly posteriorly oriented; distal end of diapophyses with a flat, slightly calcified cartilage that articulates with the ilial shaft of the pelvic girdle. Sesamoids are present on both sides of sacral diapophyses. There are two types of bony elements associated with the vertebral column: (1) spinal plates, which lie dorsal to the vertebra and are generally ornamented (except for the posteriormost ones, which might not be ornamented); and, (2) the paravertebral plates, which are associated with the transverse processes of vertebrae IV; they are poorly developed, not covering the distal part of the transverse processes, and are not ornamented. The dorsal crest of the urostyle extends for 2/3 of its length. The ilium crest extends for the whole length of this bone. Manus: Phalangeal formula of hand 1–2–3–1. The carpus is composed of a radiale, ulnare, element y fused with Carpal 2, and a large postaxial assumed to represent a fusion of centrale with Carpals 3–5. Prepollex with two elements ossified and very reduced. Tips of the terminal phalangeal elements of fingers arrow shaped. A palmar sesamoid is present. Pes: Phalangeal formula of foot 1–2–3–4–1. Tarsus composed of tibiale, fibulare, three individual elements, including distal tarsal 2–3, distal tarsal 1, element y. Distal tarsal 1 is the smallest and articulates with element y, distal tarsal 2–3, and metatarsal I and II. Distal tarsal 2–3 articulates mainly with metatarsal III, but also with metatarsal II and IV, and with distal tarsal I. Prehallux has a single element. Tips of the terminal phalangeal elements of toes II–V arrow-shaped, toes I and V reduced, digit IV elongated. Plantar and cartilage sesamoids are present in all specimens. Three sesamoids are present at the knee region, the larger one might be the graciella sesamoid.

Discussion

Osteological, bioacoustic and genetic data seem to be important to elucidate species limits, especially when considering extremely diverse lineages (*i.e.*, Monteiro et al. 2018a). *Brachycephalus herculeus* **sp. nov.** is distinguished from all its congeners based on morphological, molecular, and acoustic evidence, relying on divergence of both internal and external phenotypic traits that characterize the pumpkin toadlets. Within the *B. vertebralis* species group, a strong set of morphological characters distinguishes the new species from its sister taxon *B. bufonoides*, confirming its specific distinctness.

The genus *Brachycephalus* represents an interesting case among anurans, as it contains populations/species that are barely or not distinguishable in external morphology, yet separated by relatively deep genetic distances, as well as species that are distinct from each other morphologically but have very shallow genetic divergence (Condez et al. 2020; Folly et al. 2020, 2022; Bornschein et al. 2021; Almeida-Silva et al. 2021). The former case is frequent among the cryptically colored species with "flea-toad" phenotype, whereas the latter case occurs mainly among the brightly colored species with "pumpkin toadlet" phenotype. For example, the very similar-looking flea-toads *B. hermogenesi* and *B. sulfuratus* diverge by 10% in the 16S gene (and are not even sister species), whereas the morphologically distinct pumpkin toadlets *B. nodoterga* and *B. toby* have practically no divergence (Almeida-Silva et al. 2021). *Brachycephalus herculeus* **sp. nov.** and *B. bufonoides* represent yet another case of a sister-species pair whose members differ considerably in external appearance but present little genetic divergence (<1%).

This is even more remarkable when we consider other direct-developing taxonomic groups, such as the genera *Ischnocnema* (Gehara et al. 2013; Oswald et al. 2023), *Pristimantis* (Padial et al. 2009), *Euparkerella* (Fusinatto et al. 2013) and *Adelophryne* (Lourenço-de-Moraes et al. 2018), as well as groups with non-free living tadpoles such as *Adenomera* (Fouquet et al. 2014), which tend to exhibit high genetic distances among species. Considering the natural history and biology of species in the genus *Brachycephalus*, which are slow-moving, small-bodied and lack free-swimming larvae (traits suggestive of low dispersal ability and limited gene flow among spatially separated populations), one would expect significant genetic distances among its species. Yet, the genetic distance between *Brachycephalus herculeus* **sp. nov.** and *B. bufonoides* is similar to the ones observed among some species of *Alsodes* (Blotto et al. 2013), a group with free-living tadpoles inhabiting streams. As in previous studies (Almeida-Silva et al. 2021), we also recorded

very low genetic divergences (0.0–0.3%) among *B. pitanga*, *B. crispus* and *B. guarani* (see Table 2), despite their morphological distinctiveness. The extremely low genetic divergences among some species of pumpkin toadlets with a high number of diagnostic characters, including osteological ones, is remarkable and deserves to be further investigated. It hints at a very fast rate of morphological differentiation in the genus *Brachycephalus*, or at least in some clades within it, though for reasons not yet understood.

Many species in the genus *Brachycephalus* have increased cranial ossification while retaining a variety of juvenile features, with the neopalatine, quadratojugal and columella liable to be lost in the adults within different lineages (Trueb and Alberch 1985; Alves et al. 2006; Bornschein et al. 2016). The ancestral form of the genus is presumed to have had a miniaturized body and to have lacked paravertebral plates, and the evolution of those plates seems to be correlated with an increase in body size (Condez et al. 2020; Dos Reis et al. 2021). The absence of ornamentation on the paravertebral plates of the new species could be seen as a juvenile feature following the ontogenetic sequence of Campos et al. (2010). However, the five individuals whose skeletons were analyzed, all with mature gonads and skull presenting adult features, confirm this character as diagnostic. Such a mosaic of paedomorphic and non-paedomorphic features in the morphology of adults, as well as the intraspecific variability in the miniaturized species of *Brachycephalus* reiterates the importance of including more than one analyzed skeleton in studies of that genus (Hanken 1984; Yeh 2002).

Histological analysis of dissected individuals of *Brachycephalus darkside* shows the pigmentation in tissue following adjacent muscle fibers, *i.e.*, a connective tissue covers the dorsal musculature (epimysium) and is present between muscle fibers (perimysium and endomysium). This tissue exhibited spots of extracellular matrix containing dark pigments, which were reflected in the macroscopy of fixed specimens as well (Guimarães et al. 2017). Concerning the presence of dark-pigmented tissue within the *B. ephippium* species group, we add that there is no pigmentation in *B. ephippium*, while the black connective tissue covers all sides of dorsal muscles in *B. darkside*, and a few scattered areas with pigmentation are observed in the dorsolateral region adjacent to the dorsal musculature in *B. garbeanus* and *B. margaritatus* (Guimarães et al. 2017; Folly et al. 2021b). Within the *B. vertebralis* species group (sensu Folly et al. 2022), there is black connective tissue covering all sides of dorsal muscles in *Brachycephalus herculeus* **sp. nov.** (present study), little dark pigmentation internally around the line of the spinal vertebrae in *B. vertebralis*, and no pigmentation in *B. pitanga* (Guimarães et al. 2017). An absence of pigmentation was also observed for species of the *B. pernix* species group (*B. izecksohni* and *B. pernix*; Guimarães et al. 2017). Currently, there are still open issues regarding the intraspecific variation of dark pigmentation within each of those species, as well as information about other species in the genus *Brachycephalus*.

The geographic records for *Brachycephalus herculeus* **sp. nov.** are currently restricted to montane forests in the Parque Nacional do Desengano, located in the northern portion of the Brazilian state of Rio de Janeiro. Regarding anurofauna, this is a poorly studied region (e.g., Almeida-Gomes et al. 2010; Siqueira et al. 2011). Indeed, most studies focusing on the anurofauna of the Atlantic Rainforest of Rio de Janeiro have been conducted in the central and southern portions of the state (e.g., Carvalho-e-Silva et al. 2008, 2020; Bittencourt-Silva and Silva 2013; Dorigo et al. 2021). Due to such a lack of knowledge about the region and to the presence of poorly known preserved areas, the forests of the northern portion of Rio de Janeiro state could be promising areas for the encounter of new anuran species, as suggested by the recent discoveries of *Ischnocnema nanahallux* (Brusquetti et al. 2013), *Megaelosia* sp. (aff. *goeldii*) (De Sá et al. 2022), and *B. herculeus* **sp. nov.** (present study), all living within the limits of the protected area of Parque Estadual do Desengano.

Acknowledgments

Part of the field surveys that yielded specimens of the new species described in this work were financed by the Critical Ecosystem Partnership Fund – CEPF, Conservation International and Aliança para a Conservação da Mata Atlântica. We thank the many colleagues that assisted us during fieldwork. We also thank P Taucce for the detailed review of the manuscript. We are indebted to CFB Haddad, T Grant and RN Feio for allowing access to specimens under their care. MW Cardoso for help in laboratory. M Folly was supported by a postdoctoral fellowship from Conselho Nacional de Desenvolvimento Científico e Tecnológico (CNPq) (154743/2018-6); TH Condez was supported by fellowships from CNPq (302308/2019-9) and New Frontiers in Research Fund (NFRF Canada); THC especially thanks F Brusquetti and MTC Thomé for the assistance during the collection of specimens. JP Pombal Jr. was supported by grants from CNPq and Fundação Carlos Chagas Filho de Amparo à Pesquisa do Estado do Rio de Janeiro (FAPERJ). CFDR received grants from Conselho Nacional de Desenvolvimento Científico e Tecnológico (CNPq) (Processes Nos. 302974/2015-6, 424473/2016-0 and 304375/2020-9) and from Fundação de Amparo à Pesquisa do Estado do Rio de Janeiro (FAPERJ) through the Cientistas do Nosso Estado Program (processes Nos. E-26/202.803/2018 and E-26/201.083/2022).

References

Adobe Inc. (2019) Adobe Illustrator. Available from: https://adobe.com/products/illustrator. San Jose, California, USA.

Almeida-Gomes M, Almeida-Santos M, Goyannes-Araújo P, Borges-Júnior VNT, Vrcibradic D, Siqueira CC, Ariani CV, Dias,AS, Souza VV, Pinto RR, Van Sluys M, Rocha CFD (2010) Anurofauna of an Atlantic Rainforest fragment and its surroundings in northern Rio de Janeiro State, Brazil. Brazilian Journal of Biology 70: 871–877. https://doi.org/10.1590/S1519-69842010000400018

Almeida-Santos M, Siqueira CC, Van Sluys M, Rocha CFD (2011) Ecology of the Brazilian flea frog *Brachycephalus didactylus* (Terrarana: Brachycephalidae). Journal of Herpetology 45: 251–255. https://doi.org/10.1670/10-015.1

Almeida-Silva P, Silva-Soares T, Rodrigues MT, Verdade VK (2021) New species of flea-toad, genus *Brachycephalus* (Anura: Brachycephalidae) from the Atlantic Forest of Espírito Santo, Brazil. Zootaxa 5068: 517–532. http://doi.org/10.11646/zootaxa.5068.4.3

Altschul SF, Madden TL, Schäffer AA, Zhang J, Zhang Z, Miller W, Lipman DJ (1997) Gapped BLASTand PSI-BLAST: A new generation of protein database search programs. Nucleic Acids Research 25: 3389–3402. http://doi.org/10.1093/nar/25.17.3389

Alves ACR, Ribeiro LF, Haddad CFB, Dos Reis SF (2006) Two new species of *Brachycephalus* (Anura: Brachycephalidae) from the Atlantic Forest in Paraná State, Southern Brazil. Herpetologica 62: 221–233. https://doi.org/10.1655/05-41.1

Alves ACR, Sawaya RJ, Reis SF, Haddad CFB (2009) New Species of *Brachycephalus* (Anura: Brachycephalidae) from the Atlantic Rain Forest in São Paulo State, Southeastern Brazil. Journal of Herpetology 43: 212–219. https://doi.org/10.1670/0022-1511-43.2.212

Audacity Team (2017) Audacity: Free Audio Editor and Recorder, Version 2.2.1. Available at https://www.audacityteam.org. Carnegie Mellon University, USA.

Bioacoustics Research Program. 2014. Raven Pro: Interactive Sound Analysis Software, Version 1.5. The Cornell Lab of Ornithology, Ithaca, NY. Available at https://ravensoundsoftware.com.

Bittencourt-Silva GB, da Silva HR (2013) Insular anurans (Amphibia: Anura) of the coast of Rio de Janeiro, Southeast, Brazil. Check List 9: 225–234. https://doi.org/10.15560/9.2.225

Blotto B, Nuñez JJ, Basso NG, Úbeda CA, Wheeler WC, Faivovich J (2013) Phylogenetic relationships of a Patagonian frog radiation, the *Alsodes* + *Eupsophus* clade (Anura: Alsodidae), with comments on the supposed paraphyly of *Eupsophus.* Cladistics 29: 113–131. https://doi.org/10.1111/j.1096-0031.2012.00417.x

Bornschein MR, Ribeiro LF, Blackburn DC, Stanley EL, Pie MR (2016) A new species of *Brachycephalus* (Anura: Brachycephalidae) from Santa Catarina, southern Brazil. PeerJ 4: e2629. https://doi.org/10.7717/peerj.2629

Bornschein MR, Ribeiro LF, Rollo MM, Confetti AE, Pie MR (2018) Advertisement call of *Brachycephalus albolineatus* (Anura: Brachycephalidae). PeerJ 6: e5273. https://doi.org/10.7717/peerj.5273

Bornschein MR, Rollo MM, Pie MR, Confetti AE, Ribeiro LF (2019) Redescription of the advertisement call of *Brachycephalus tridactylus* (Anura: Brachycephalidae). Phyllomedusa 18: 3 –12. https://doi.org/10.11606/issn.2316-9079.v18i1p3-12

Bornschein MR, Ribeiro LF, Teixeira L, Belmonte-Lopes R, Moraes LA de, Corrêa L, Maurício GN, Nadaline J, Pie MR (2021) A review of the diagnosis and geographical distribution of the recently described flea toad *Brachycephalus sulfuratus* in relation to *B. hermogenesi* (Anura: Brachycephalidae). PeerJ 9: e10983. https://doi.org/10.7717/peerj.10983

Brusquetti F, Thomé MTC, Canedo C, Condez TH, Haddad CF (2013) A new *Ischnocnema* (Brachycephalidae) from northern Rio de Janeiro, Brazil. Herpetologica 69: 175–185. https://doi.org/10.1655/HERPETOLOGICA-D-12-00050

Campos LA, Silva HR, Sebben A (2010) Morphology and development of additional bony elements in genus *Brachycephalus* (Anura: Brachycephalidae). Biological Journal of the Linnean Society 99: 752–767. https://doi.org/10.1111/j.1095-8312.2010.01375.x

Carvalho-e-Silva AMT, Silva GR, Carvalho-e-Silva SP (2008) Anuros da Reserva Rio das Pedras, Mangaratiba, RJ, Brazil. Biota Neotropica 8: 199–209. https://doi.org/10.1590/S1676-06032008000100021

Carvalho-e-Silva SP, Carvalho-e-Silva AMPT, Folly M, Luna-Dias C, Bezerra AM, Gomes MR, Caram J., Peixoto OL, Izecksohn E (2020) Parque Nacional da Serra dos Órgãos: Highest amphibian diversity with an Atlantic Forest protected area. Biota Neotropica 20: e20201033. https://doi.org/10.1590/1676-0611-BN-2020-1033

Cei JM (1980) Amphibians of Argentina. Monitore Zoologico Italiano. Nuova Serie, Monographs 2. Universita degli studi di Firenze, Florence.

Clemente-Carvalho RB, Klaczko J, Perez SI, Alves AC, Haddad CF, dos Reis SF (2011) Molecular phylogenetic relationships and phenotypic diversity in miniaturized toadlets, genus *Brachycephalus* (Amphibia: Anura: Brachycephalidae). Molecular Phylogenetics and Evolution 61: 79–89. https://doi.org/10.1016/j.ympev.2011.05.017

Clemente-Carvalho RBG, Giaretta AA, Condez TH, Haddad CFB, dos Reis SF (2012) A New species of miniaturized toadlet, genus *Brachycephalus* (Anura: Brachycephalidae), from the Atlantic Forest of Southeastern Brazil. Herpetologica 68: 365–374. https://doi.org/10.1655/HERPETOLOGICA-D-11-00085.1

Clemente-Carvalho RBG, Perez SI, Tonhatti CH, Condez, TH, Sawaya RJ, Haddad CFB, and Dos Reis SF (2016) Boundaries of morphological and molecular variation and distribution of a miniaturized froglet, *Brachycephalus nodoterga* (Anura: Brachycephalidae). Journal of Herpetology 50: 169–178. http://dx.doi.org/10.1670/14-119

Condez TH, Clemente-Carvalho RBG, Haddad CFB, dos Reis SF (2014) A new species of *Brachycephalus* (Anura: Brachycephalidae) from the highlands of the Atlantic Forest, Southeastern Brazil. Herpetologica 70: 89–99. https://doi.org/10.1655/HERPETOLOGICA-D-13-00044

Condez TH, Haddad CFB, Zamudio KR (2020) Historical biogeography and multi-trait evolution in miniature toadlets of the genus *Brachycephalus* (Anura: Brachycephalidae). Biological Journal of the Linnean Society 129: 664–686. https://doi.org/10.1093/biolinnean/blz200

Condez TH, Monteiro JP, Comitti EJ, Garcia PC, Amaral IB, Haddad CF (2016) A new species of flea-toad (Anura: Brachycephalidae) from southern Atlantic Forest, Brazil. Zootaxa 4083: 40–56. https://doi.org/10.11646/zootaxa.4083.1.2

Condez TH, Monteiro JPC, Malagoli LC, Trevine, VC, Schunck F, Garcia PCA, Haddad, CFB (2021) Notes of the hyperossified pumpkin toadlets of the genus *Brachycephalus* (Anura: Brachycephalidae) with the description of a new species. Herpetologica 77: 176–194. https://doi.org/10.1655/HERPETOLOGICA-D-20-00031

Darst CR, Cannatella DC (2004) Novel relationships among hyloid frogs inferred from 12S and 16S mitochondrial DNA sequences. Molecular Phylogenetics and Evolution 31: 462–475. http://doi.org/10.1016/j.ympev.2003.09.003

De Sá FP, Condez TH, Lyra ML, Haddad CFB, Malagoli LR (2022) Unveiling the diversity of Giant Neotropical Torrent frogs (Hylodidae): Phylogenetic relationships, morphology, and the description of two new species. Systematics and Biodiversity 20: 1–31. https://doi.org/10.1080/14772000.2022.2039318

Dorigo TA, Siqueira CC, Oliveira JCF, Fusinatto LA, Santos-Pereira M, Almeida-Santos M, Maia-Carneiro T, Reis CNC, Rocha CFD (2021) Amphibians and reptiles from the Parque Nacional da Tijuca, Brazil, one of the world's largest urban forests. Biota Neotropica 21: e20200978. https://doi.org/10.1590/1676-0611-BN-2020-0978

Dos Reis SF, Clemente-Carvalho RBG, Dos Santos CMSFF, Lopes RT, Von Zuben FJ, Laborda PR, Perez SI (2021) Skull diversity and evolution in miniaturized amphibians, genus *Brachycephalus* (Anura: Brachycephalidae). Anatomical Record 304: 1329–1343. https://doi.org/10.1002/ar.24554

Duellman WE (1970) Hylid frogs of Middle America, Volumes 1 and 2. Monograph of the Museum of Natural History. University of Kansas, Lawrence, KS, xi + 753 pp., 72 plates.

Fabrezi M (1992) El carpo de los anuros. Alytes 10: 1–29.

Fabrezi M (1993) The anuran tarsus. Alytes 11: 47–63.

Fabrezi M (2001) A survey of prepollex and prehallux variation in anuran limbs. Zoological Journal of the Linnean Society 131: 227–248. https://doi.org/10.1111/j.1096-3642.2001.tb01316.x

Fabrezi M, Alberch P (1996) The carpal elements of anurans. Herpetologica 52: 188–204.

Firkowski CR, Bornschein MR, Ribeiro LF, Pie MR (2016) Species delimitation, phylogeny and evolutionary demography of co-distributed, montane frogs in the southern Brazilian Atlantic Forest. Molecular Phylogenetics and Evolution 100: 345–360. https://doi.org/10.1016/j.ympev.2016.04.023

Folly M, Amaral LC, Carvalho-e- Silva SP, Pombal Jr JP (2020) Rediscovery of the toadlet *Brachycephalus bufonoides* Miranda-Ribeiro, 1920 (Anura: Brachycephalidae) with osteological and acoustic descriptions. Zootaxa 4819: 265–294. https://doi.org/10.11646/zootaxa.4819.2.3

Folly M, Luna-Dias C, Miguel IR, Ferreira Jr, JC, Machado A, Lopes RT, Pombal Jr, JP (2021a) Tiny steps towards greater knowledge: An osteological review with novel data on the Atlantic Forest toadlet of the *Brachycephalus ephippium* species group. Acta Zoologica 104: 71–105. https://doi.org/10.1111/azo.12398

Folly M, Woitovicz-Cardoso M, Canedo C, Nogueira-Costa P, Pombal Jr, JP (2021b) How long does it take to know a species? Redescription, vocalization, and chigger mites infestation pattern in the centenary *Brachycephalus garbeanus* (Anura: Brachycephalidae). Zootaxa 4950: 321–344. https://doi.org/10.11646/zootaxa.4950.2.5

Folly M, Vrcibradic D, Siqueira CC, Rocha CFB, Machado AA, Lopes RT, Pombal Jr, JP (2022) A new species of *Brachycephalus* (Anura, Brachycephalidae) from a montane Atlantic Rainforest of southeastern Brazil, with a reappraisal of the species group in the genus. Ichthyology & Herpetology 110: 585–601. http://doi.org/10.1643/h2020144

Fouquet ACS. Cassini CS. Haddad CFB, Pech N, Rodrigues MT 2014. Species delimitation, patterns of diversification and historical biogeography of the Neotropical frog genus *Adenomera* (Anura, Leptodactylidae). Journal of Biogeography 41: 855–870. https://doi.org/10.1111/jbi.12250

Frost DR (2023) Amphibian Species of the World: An Online Reference. Version 6.1. American Museum of Natural History. https://amphibiansoftheworld.amnh.org [accessed 24 September 2023].

Fusinatto LA, Alexandrino J, Haddad CFB, Brunes TO, Rocha CFD, Sequeira F (2013) Cryptic genetic diversity is paramount in small-bodied amphibians of the genus *Euparkerella* (Anura: Craugastoridae) endemic to the Brazilian Atlantic Forest. PLoS ONE 8: e79504. https://doi.org/10.1371/journal.pone.0079504

Garey MV, Lima AMX, Hartmann MT, Haddad CFB (2012) A new species of miniaturized toadlet, genus *Brachycephalus* (Anura: Brachycephalidae), from southern Brazil. Herpetologica 68: 266–271. https://doi.org/10.1655/HERPETOLOGICA-D-11-00074.1

Gehara M, Canedo C, Haddad CFB, Vences M. (2013) From widespread to microendemic: Molecular and acoustic analyses show that *Ischnocnema guentheri* (Amphibia: Brachycephalidae) is endemic to Rio de Janeiro, Brazil. Conservation Genetics 14: 973–982. https://doi.org/10.1007/s10592-013-0488-5

Giaretta AA, Sawaya R (1998) Second species of *Psyllophryne* (Anura: Brachycephalidae). Copeia 1998: 985–987. https://doi.org/10.2307/1447345

Goebel AM, Donnelly JM, Atz ME (1999) PCR primers and amplification methods for 12S ribosomal DNA, the control region, cytochrome oxidase I, and cytochrome b in bufonids and other frogs, and an overview of PCR primers which have amplified DNA in amphibians successfully. Molecular Phylogenetics and Evolution 11: 163–199. https://doi.org/10.1006/MPEV.1998.0538

Guimarães CS, Luz S, Rocha PC, Feio RN (2017) The dark side of pumpkin toadlet: A new species of *Brachycephalus* (Anura: Brachycephalidae) from Serra do Brigadeiro, southeastern Brazil. Zootaxa 4258: 327–344. https://doi.org/10.11646/zootaxa.4258.4.2

Haddad CDB, Toledo LF, Prado CPA, Loebmann D, Gasparini JL, Sazima I (2013) Guia dos anfíbios da Mata Atlântica: Diversidade e biologia. Anolisbooks, São Paulo.

Haddad CFB, Alves ACR, Clemente-Carvalho RBG, dos Reis SF (2010) A new species of *Brachycephalus* from the Atlantic Rain Forest in São Paulo State, southeastern Brazil (Amphibia: Anura: Brachycephalidae). Copeia 2010: 410–420. https://doi.org/10.1643/CH-09-102

Hanken J (1984) Miniaturization and its effects on cranial morphology in plethodontid salamanders, genus *Thorius* (Amphibia: Plethodontidae). I. Osteological variation. Biological Journal of the Linnean Society 23: 55–75. https://doi.org/10.1111/j.1095-8312.1984.tb00806.x

Hedges SB, Duellman WE, Heinicke MP (2008) New World direct-developing frogs (Anura: Terrarana): Molecular phylogeny, classification, biogeography, and conservation. Zootaxa 1737: 1–182. https://doi.org/10.11646/zootaxa.1737.1.1

Heinicke MP, Lemmon AR, Lemmon EM, McGrath K, Hedges SB (2018) Phylogenomic support for evolutionary relationships of New World direct-developing frogs (Anura: Terraranae). Molecular Phylogenetics and Evolution 118: 145–155. https://doi.org/10.1016/j.ympev.2017.09.021

Hepp F, Pombal Jr JP (2019) Naming structures and qualifying properties of anuran bioacoustical signals: A call for a homology-based nomenclature and equality for quantitative data. Anais da Academia Brasileira de Ciências 91: e20190965. https://doi.org/10.1590/0001-3765201920190965

Heyer WR, Rand AS, Cruz CAG, Peixoto OL, Nelson CE (1990) Frogs of Boraceia. Arquivos de Zoologia 41: 231–410.

Izecksohn E (1971) Nôvo gênero e nova espécie de Brachycephalidae do estado do Rio de Janeiro, Brasil (Amphibia, Anura). Boletim do Museu Nacional. Nova Serie, Zoologia 280: 1–12.

Kaplan M (2002) Histology of the anteroventral part of the breast-shoulder apparatus of *Brachycephalus ephippium* (Brachycephalidae) with comments on the validity of the genus *Psyllophryne* (Brachycephalidae). Amphibia-Reptilia 23: 225–227. https://doi.org/10.1163/156853802760061840

Katoh K, Standley DM (2013) MAFFT multiple sequence alignment software version 7: Improvements in performance and usability. Molecular Biology and Evolution 30: 772–780. https://dx.doi.org/10.1093/molbev/mst010

Katoh K, Toh H (2008) Improved accuracy of multiple ncRNA alignment by incorporating structural information into a MAFFT-based framework. BMC Bioinformatics 9: 212. https://dx.doi.org/10.1186/1471-2105-9-212

Köhler J, Jansen M, Rodríguez A, Kok PJR, Toledo LF, Emmrich M, Glaw F, Haddad CFB, Rödel MO, Vences M (2017) The use of bio-

acoustics in anuran taxonomy: Theory, terminology, methods and recommendations for best practice. Zootaxa 4251: 1–124. http://dx.doi.org/10.11646/zootaxa.4251.1.1

Kumar S, Stecher G, Li M, Knyaz C, Tamura K (2018) MEGA X: Molecular Evolutionary Genetics Analysis across computing platforms. Molecular Biology and Evolution 35: 1547–1549. https://doi.org/10.1093/molbev/msy096

Lanfear R, Frandsen PB, Wright AM, Senfeld T, Calcott B. (2017) Partitionfinder 2: New methods for selecting partitioned models of evolution for molecular and morphological phylogenetic analyses. Molecular Biology and Evolution 34: 772–773. https://dx.doi.org/10.1093/molbev/msw260

Lourenço-de-Moraes R, Dias IR, Mira-Mendes CV, Oliveira RMD, Barth A, Ruas DS, Vences M, Solé M, Bastos RP (2018) Diversity of miniaturized frogs of the genus *Adelophryne* (Anura: Eleutherodactylidae): A new species from the Atlantic Forest of northeast Brazil. PLoS ONE 13: e0201781. https://doi.org/10.1371/journal.pone.0201781

Lyra ML, Monteiro JPC, Rancilhac L, Irisarri I, Künzel S, Sanchez E, Condez TH, Rojas-Padilla O, Solé M, Toledo LF, Haddad CFB, Vences M (2021) Initial phylotranscriptomic confirmation of homoplastic evolution of the conspicuous coloration and bufoniform morphology of pumpkin-toadlets in the genus *Brachycephalus*. Toxins 13: 816. https://doi.org/10.3390/toxins13110816

Mângia S, Santana DJ, Drummond LO, Sabagh LT, Ugioni L, Nogueira-Costa P, Wachlevski M (2023) A new species of *Brachycephalus* (Anura: Brachycephalidae) from Serra do Tabuleiro, southern Brazil. Vertebrate Zoology 73: 575–597. https://doi.org/10.3897/vz.73.e102098

Miller MA, Pfeiffer W, Schwartz T (2010) Creating the CIPRES Science Gateway for Inference of Large Phylogenetic Trees. Proceedings of the Gateway Computing Environments Workshop 2010: 1–8. https://dx.doi.org/10.1109/GCE.2010.5676129

Monteiro JP, Condez TH, Garcia PCA, Comitti EJ, Amaral IB, Haddad CFB (2018a) A new species of *Brachycephalus* (Anura, Brachycephalidae) from the coast of Santa Catarina State, southern Atlantic Forest, Brazil. Zootaxa 4407: 483–505. https://doi.org/10.11646/zootaxa.4407.4.2

Monteiro JP, Condez TH, Garcia PCA, Haddad CFB (2018b) The advertisement calls of two species of *Brachycephalus* (Anura: Brachycephalidae) from southern Atlantic Forest, Brazil. Zootaxa 4415: 183–188. https://doi.org/10.11646/zootaxa.4415.1.10

Moritz C, Schneider CJ, Wake DB (1992) Evolutionary relationships within the *Ensatina eschscholtzii* complex confirm the ring species interpretation. Systematic Biology 41: 273–291. https://doi.org/10.1093/sysbio/41.3.273

Napoli MF, Caramaschi U, Cruz CAG, Dias IR (2011) A new species of flea-toad, genus *Brachycephalus* Fitzinger (Amphibia: Anura: Brachycephalidae), from the Atlantic rainforest of southern Bahia, Brazil. Zootaxa 2739: 33–40. https://doi.org/10.11646/zootaxa.2739.1.3

Nunes I, Guimarães CS, Moura PHAG, Pedrozo M, Moroti M de T, Castro LM, Stuginski DR, Muscat, E (2021) Hidden by the name: A new fluorescent pumpkin toadlet from the *Brachycephalus ephippium* group (Anura: Brachycephalidae). PLoS ONE 16: e0244812. http://doi.org/10.1371/journal.pone.0244812

Oliveira EG, Haddad CFB (2017) Activity, acoustic repertoire and social interactions of the Red Toadlet, *Brachycephalus pitanga* (Anura: Brachycephalidae). Salamandra 53: 501–506.

Oswald CB, Magalhães RF, Garcia PCA, Santos FR, Neckel-Oliveira S (2023) Integrative species delimitation helps to find the hidden diversity of the leaf-litter frog *Ischnocnema manezinho* (Garcia, 1996) (Anura, Brachycephalidae), endemic to the southern Atlantic Forest. PeerJ 11: e15393. https://doi.org/10.7717/peerj.15393

Padial JM, Castroviejo-Fisher S., Köhler J, Vila C, Chaparro JC, de la Riva I (2009) Deciphering the products of evolution at the species level: The need for an integrative taxonomy. Zoologica Scripta 38: 431–447. https://doi.org/10.1111/j.1463-6409.2008.00381.x

Padial JM, Grant T, Frost DR (2014) Molecular systematics of terraranas (Anura: Brachycephaloidea) with an assessment of the effects of alignment and optimality criteria. Zootaxa 3825: 1–132. https://doi.org/10.11646/zootaxa.3825.1.1

Pie MR, Ribeiro LF (2015) A new species of *Brachycephalus* (Anura: Brachycephalidae) from the Quiriri mountain range of southern Brazil. PeerJ 3: e1179. https://doi.org/10.7717/peerj.1179

Pie MR, Ribeiro LF, Confetti AE, Nadaline MJ, Bornschein MR (2018) A new species of *Brachycephalus* (Anura: Brachycephalidae) from southern Brazil. PeerJ 6: e5683. https://doi.org/10.7717/peerj.5683

Pombal JP (2010) A posição taxonômica das "variedades" de *Brachycephalus ephippium* (Spix, 1824) descritas por Miranda-Ribeiro, 1920 (Amphibia, Anura, Brachycephalidae). Boletim do Museu Nacional (Nova Serie, Zoologia) 526: 1–12.

Pombal JP, Gasparini JL (2006) A new *Brachycephalus* (Anura: Brachycephalidae) from the Atlantic Rainforest of Espírito Santo, southeastern Brazil. South American Journal of Herpetology 1: 87–93. https://doi.org/10.2994/1808-9798

Pombal JP, Izecksohn E (2011) Uma nova espécie de *Brachycephalus* (Anura, Brachycephalidae) do estado do Rio de Janeiro. Papéis Avulsos de Zoologia 51: 443–451. https://doi.org/10.1590/S0031-10492011002800001

Pombal JP., Sazima I, Haddad, CFB (1994) Breeding behavior of the pumpkin toadlet, *Brachycephalus ephippium* (Brachycephalidae). Journal of Herpetology 28: 519–519. https://doi.org/10.2307/1564972

Pombal JP, Wistuba EM, Bornschein MR (1998) A new species of brachycephalid (Anura) from the Atlantic Rain Forest of Brazil. Journal of Herpetology 32: 70–74. https://doi.org/10.2307/1565481

R Core Team (2022) R: A Language and Environment for Statistical Computing. R Foundation for Statistical Computing, Vienna. Available at https://www.r-project.org

Rambaut A (2016) FigTree v.1.4.3 tree Figure Drawing Tool. University of Edinburgh, Edinburgh. http://tree. bio. ed. ac. uk/software/figtree.

Rambaut A, Suchard MA, Xie D, Drummond AJ (2014) Tracer v1.6. University of Edinburgh, Edinburgh. Available at https://tree.bio.ed.ac.uk/software/figtree.

Ribeiro LF, Alves ACR, Haddad CFB, dos Reis SF (2005) Two new species of *Brachycephalus* Günther, 1858 from the state of Paraná, southern Brazil (Amphibia: Anura: Brachycephalidae). Boletim do Museu Nacional. Nova Serie, Zoologia 519: 1–18

Ribeiro LF, Blackburn DC, Stanley EL, Pie MR, Bornschein MR (2017) Two new species of the *Brachycephalus pernix* group (Anura: Brachycephalidae) from the state of Paraná, southern Brazil. PeerJ 5: e3603. https://doi.org/10.7717/peerj.3603

Ribeiro LF, Bornschein MR, Belmonte-Lopes R, Firkowski CR, Morato SA, Pie MR (2015) Seven new microendemic species of *Brachycephalus* (Anura: Brachycephalidae) from southern Brazil. PeerJ 3: e1011. https://doi.org/10.7717/peerj.1011

Ronquist F, Teslenko M, van der Mark P, Ayres DL, Darling A, Höhna S, Larget B, Liu L, Suchard MA, Huelsenbeck JP (2012) MrBayes 3.2: Efficient Bayesian phylogenetic inference and model choice across a large model space. Systematic Biology 61: 539–542. https://dx.doi.org/10.1093/sysbio/sys029

Sabaj, MH (2016) Standard Symbolic Codes for Institutional Resource Collections in Herpetology and Ichthyology: An Online Reference, Version 6.5. American Society of Ichthyologists and Herpetologists. Available at https://www.asih.org.

Siqueira CC, Vrcibradic D, Almeida-Gomes M, Menezes VA, Borges-Junior VNT, Hatano FH, Pontes JAL, Goyannes-Araújo P, Guedes DM, Van Sluys M, Rocha CFD (2011) Species composition and density estimates of the anurofauna of a site within the northernmost large Atlantic Forest remnant (Parque Estadual do Desengano) in the state of Rio de Janeiro, Brazil. Biota Neotropica 11: 131–137.

Stecher G, Tamura K, Kumar S (2020) Molecular Evolutionary Genetics Analysis (MEGA) for macOS. Molecular Biology and Evolution 37: 1237–1239. https://doi.org/10.1093/molbev/msz312

Sueur J, Aubin T, Simonis C (2008) Seewave, a free modular tool for sound analysis and synthesis. Bioacoustics 18: 213–226. http://dx.doi.org/10.1080/09524622.2008.9753600

Taylor WR, Van Dyke G (1985) Revised procedures for staining and clearing small fishes and other vertebrates for bone and cartilage study. Cybium 9: 107–119.

Trewavas E (1933) The hyoid and larynx of the Anura. Philosophical Transactions of the Royal Society B 222: 401–527. https://doi.org/10.1098/rstb.1932.0020

Trueb L (1973) Bones, frogs, and evolution. In: Vial JL (Ed.) Evolutionary Biology of the Anurans: Contemporary Research on Major Problems. University of Missouri Press, Columbia, MO, 65–132.

Trueb L (2015) Osteology. In: Duellman WE (Ed.) Marsupial Frogs: *Gastrotheca* and Allied Genera; with Osteology. Johns Hopkins University Press, Baltimore, MD, 31–51.

Trueb L, Alberch P (1985) Miniaturization and the anuran skull: A case study of heterochrony. In: Dunker HR, Fleischer G (Eds) Functional Morphology of the Vertebrates. Gustav Fischer Verlag, New York, NY, 113–121.

Vaidya G, Lohman DJ, Meier R (2011) SequenceMatrix: Concatenation software for the fast assembly of multi-gene datasets with character set and codon information. Cladistics 27: 171–180. https://doi.org/10.1111/j.1096-0031.2010.00329.x

Verdade, VK, Rodrigues MT, Cassimiro J, Pavan D, Liou M, Lange MC (2008) Advertisement call, vocal activity, and geographic distribution of *Brachycephalus hermogenesi* (Giaretta & Sawaya, 1998) (Anura, Brachycephalidae). Journal of Herpetology 42: 542–549. https://doi.org/10.1670/07-287.1

Yeh J (2002) The effect of miniaturized body size on skeletal morphology in frogs. Evolution 56: 628–641. https://doi.org/10.1111/j.0014-3820.2002.tb01372.x

Supplementary Material 1

Table S1

Authors: Folly M, Condez TH, Vrcibradic D, Rocha CFD, Machado AS, Lopes RT, Pombal Jr JP (2024)
Data type: .pdf
Explanation note: Specimens examined with their respective brazilian localities.

Link: https://doi.org/vz.74.e103573.suppl1

Supplementary Material 2

Table S2

Authors: Folly M, Condez TH, Vrcibradic D, Rocha CFD, Machado AS, Lopes RT, Pombal Jr JP (2024)
Data type: .pdf
Explanation note: List of voucher specimens included in molecular analysis, locality data, GenBank accession numbers, and references. Specimens in bold refer to the new sequences generated in this study. Brazilian state abbreviations are as follows: BA, Bahia; ES, Espírito Santo; MG, Minas Gerais; RJ, Rio de Janeiro; SC, Santa Catarina; PR, Paraná; SP, São Paulo..

Link: https://doi.org/vz.74.e103573.suppl2